Environmental Science and Pollution Research (2023) 30:12741–12768
https://doi.org/10.1007/s11356-022-23006-8

RESEARCH ARTICLE

Human carcinogenic risk analysis and utilization of shale gas water-based drilling cuttings in road materials

Chao-qiang Wang[1,2,3] · Shen Chen[4] · De-ming Huang[1] · Qi-cong Huang[3] · Min-jie Tu[5] · Kai Wu[6] · Yan-yan Liu[1]

Received: 21 June 2022 / Accepted: 8 September 2022 / Published online: 17 September 2022

Abstract

Water-based drilling cuttings (WDC) generated during shale gas development will endanger human health and ecological security. The modern analytical techniques are used to analyze the organic pollutants in WDC, and the human health and ecological security risks of harmful pollutants in WDC under specific scenarios are evaluated. The results showed that the content of organic pollutants in WDC was evaluated by human health and safety risk assessment. The comprehensive carcinogenic risks of all exposure pathways of single pollutant benzo(a)anthracene, benzo(a)pyrene, benzo(k)fluoranthene, and indeno(1,2,3-cd)pyrene were acceptable. However, the cumulative carcinogenic risk of exposure to dibenzo(a,h)anthracene particles via skin exposure was not acceptable. It was considered that only dibenzo(a,h)anthracene had carcinogenic effect, and the risk control limit of dibenzo(a,h)anthracene in WDC was 1.8700 mg/kg by calculation. As well as, the "WDC-cement" gel composite structure was deeply analyzed, and the physical and chemical properties and mechanism of organic pollutants in cement solidified WDC were analyzed, which provided theoretical support for the study of WDC pavement cushion formula. Based on the above conclusions and combined with the actual site, by studying and adjusting the formula of WDC pavement cushion, the WDC pavement cushion was finally designed by 6% cement + 50% WDC + 44% crushed stone. The 7d unconfined compressive strength met the requirements of the Chinese standard "*Technical Guidelines for Construction of Highway Roadbases*" (JTG/T F20-2015). Also, the process route of WDC as road cushion product was sampled and analyzed. In addition, the leaching concentration of main pollutants all met the relevant standards of China. Therefore, this study can provide a favorable way for the efficient, safe, and environmentally friendly utilization of WDC, and ensure the ecological environment safety and human health safety of WDC in resource utilization.

Keywords WDC · Human health · Risk assessment · Road materials

Responsible Editor: Guilherme L. Dotto

✉ Kai Wu
wukai@tongji.edu.cn

[1] School of Material Science and Engineering, Chongqing Jiaotong University, Chongqing 400074, China

[2] Chongqing Haopan Energy Saving Technology Co., Ltd, Chongqing 401329, China

[3] Chongqing Institute of Modern Construction Industry Development, Chongqing 400066, China

[4] School of Civil Engineering, Chongqing Jiaotong University, Chongqing 400074, China

[5] CSCEC Strait Construction and Development Co., Ltd, Fuzhou 350015, China

[6] Key Laboratory of Advanced Civil Engineering Materials of Ministry of Education, School of Materials Science and Engineering, Tongji University, Shanghai 201804, China

Introduction

The outbreak of the coronavirus disease (COVID-19) in late 2019 has had a great impact on the global economy. Due to the close ties around the world, the COVID-19 epidemic leads to the global supply chain rupture, which leads to a new round of global energy crisis. The epidemic is also expected to have a lasting impact on future global energy needs (Wang and Su 2020; Hu et al. 2022). At the same time, human activities have intensified global climate change. If greenhouse gas emissions such as carbon dioxide are not strictly controlled, the global temperature in the twenty-first century will rise by more than 2 °C, which will have a serious impact on human society and the natural environment (Wang and Xiong 2021; Li et al. 2022). Reducing greenhouse gas emissions is the common responsibility of all mankind. Therefore, it is urgent to find an efficient and clean

energy to meet the current global energy demand. With the increasing depletion of fossil fuels such as coal and oil, shale gas resources have broad development prospects worldwide.

China is a country with abundant shale gas resources. Shale gas refers to the natural gas enriched in the shale rich in organic matter, which is dominated by thermal maturity cracking or biological action and the interaction between the two. It has high calorific value and is a very efficient and green clean energy with broad market prospects and economic value (Li et al. 2020a, b; Wang et al. 2018a, b, c, d). However, in the process of shale gas development and utilization, large amounts of water-based drilling cuttings (WDC) are produced. It is necessary to use water-based drilling fluid to drill to about 1800 m in the drilling process of the second horizontal section of shale gas, and the waste returned to the ground is WDC (Wang and Xiong 2021, Wang et al. 2014). Its composition mainly includes expansive soil, lubricant, pure alkali, KCl, and heavy metals. Its composition is complex, and easy to cause pollution to the environment. Therefore, it is urgent to dispose of WDC safely and environmentally. At present, some studies only focus on the alternative methods of resource utilization of these wastes in the resource utilization of WDC, such as the production of building materials, such as bricks (George and Antonis 2021; Mojtaba et al. 2020; Symeonides et al. 2019; Ayati et al. 2019; Dai et al. 2019), concrete (Yang et al. 2021; Mohsen et al. 2021; Li et al. 2020a, b; Amelung al. 2020; Ma et al. 2019), aggregates (Bamdad et al. 2019; Siddique et al. 2021; Sundis et al. 2021; Moreno-Maroto et al. 2018; Prachasaree et al. 2020), glass materials (Baino and Ferraris 2019; Stoch et al. 2018; Grilo et al. 2019; Alves et al. 2017), slag-red mud cementitious materials (Ban et al. 2018; Faried et al. 2021; Mymrin et al. 2017; Ye et al. 2017), and ceramic materials (Sun et al. 2021; Cheng et al. 2018; Ren et al. 2019; Cao et al. 2019).

The study of sintered bricks is to use WDC as a partial substitute material and heat treatment method to heat the waste at high temperature to induce coherent bonding or welding of adjacent particles, so as to gain dense products with lower porosity and make the physical, mechanical, and environmental properties of WDC sintered bricks meet the corresponding Chinese standards and ASTM standards requirements (Liu et al. 2021; Li et al. 2019; Luo et al. 2020). The research of concrete is mainly based on the physical and chemical properties of WDC. Shale gas WDC is used as siliceous and calcareous materials to improve the physical and chemical properties of concrete. At the same time, a new WDC resource utilization technology is developed (Wang and Xiong 2021; Ghorbani et al. 2019; Jiang et al. 2020). The research on aggregate mainly focuses on the applicability of different types of secondary materials as artificial lightweight aggregate. In addition to the commonly used materials (such as clay and fly ash) for aggregate production, various types of waste can be used as alternative materials (Piszcz-Karaś et al. 2019; Burciaga-Díaz et al. 2020; Amin et al. 2021). The research of glass materials is mainly based on the mixture of kaolin and oil well drilling waste as raw materials. The recycled raw materials (waste) are mixed with commercial materials to adjust the composition of glass, and glass–ceramic precursor materials are obtained by melting. The obtained vitreous powder is studied by thermal, chemical, and structural characterization techniques. The pellets were pressed and sintered to obtain glass–ceramic materials (Danielle et al. 2019; Stoch et al. 2018; Mohajerani et al. 2019). The research on slag-red mud cementing material mainly uses waste drilling fluid, blast furnace slag, and red mud as raw materials to prepare a new type of cementing material, aiming at achieving an environmentally friendly and efficient solution for waste recycling. Meanwhile, the physical and chemical properties of slag-red mud cementitious materials were evaluated by compressive strength, X-ray diffraction analysis, and mercury intrusion porosimetry (Cheng et al. 2019; Wang et al. 2018a, b, c, d). In the study of ceramic materials, spinel-corundum ceramics were prepared from ferrochrome slag and bauxite. The sintering behavior of spinel corundum ceramics is preliminarily analyzed. In addition, the liquid phase process is modified by adding pyrolusite in the ceramic system to obtain high strength ceramics (Shao et al. 2022; Fan et al. 2021). In summary, the above studies added binders (such as Portland cement, fly ash, and lime) to WDC to effectively fix pollutants through chemical fixation and physical coating. The cured WDC is buried on site or transferred to other sites for final disposal. Obviously, this process is mainly a process of fixing pollutants rather than completely damaging pollutants, which may release and pollute soil and groundwater in the future.

Although domestic and international conventional oilfield WDC (Abdul-Wahab et al. 2020; Burghard et al. 2021; Xie et al. 2020; Maziar et al. 2018; Notani et al. 2019, Bedia et al. 2018; Burciaga-Díaz et al. 2020; Wang et al. 2017a, b; Allwood 2018; Ghorbani et al. 2019) has a lot of research on resource utilization, but there are still many problems in risk control of resource products. (1) Presently, there is no uniform and systematic testing method for resource products. (2) There is no unified pollution control standard for comprehensive utilization of shale gas cuttings. (3) Long-term use safety performance of resource products cannot be guaranteed. Moreover, the physicochemical properties and pollution characteristics of shale gas WDC are different from those of ordinary oilfield WDC, so it cannot play a targeted guiding role in the resource utilization of shale gas WDC. Based on the above problems of resource products, this paper puts forward reasonable suggestions.

Therefore, the innovation of this paper is to use the human health safety risk assessment method to evaluate the safety of

organic pollutants in WDC, and to construct the evaluation model of human health and ecological safety risk assessment. In this paper, the harmful organic pollutants in WDC solid phase were systematically studied and analyzed by modern analysis technology, and the release and migration characteristics of organic pollutants in WDC in various environmental media were comprehensively analyzed. The human health and safety risk assessment method was used to evaluate the safety of organic pollutants in WDC, and the evaluation model of human health and ecological safety risk assessment was constructed. The pollution control indexes and limits of WDC resource utilization were obtained by calculation, which laid a solid foundation for its resource utilization. Based on the above research conclusions and filed reality, a method for efficient utilization of shale gas WDC road materials is proposed, and the curing mechanism of "WDC-cement" gel composite structure in WDC road materials is deeply analyzed to further improve the environmental safety of WDC resource products. The above research results will further promote the basic technology research of shale gas WDC resource utilization, and provide a favorable way for the efficient, safe, and environmentally friendly utilization of WDC.

Experiments

Raw materials

The Portland cement 42.5 (P.O 42.5) is available from a Chongqing Cement Co., Ltd (China). WDC is in a powdered form (after drying) and the particle medium diameter is 42 μm, and is given by a shale gas field in Chongqing city, China.

The selection of WDC samples fully considers the characteristics of solid waste raw materials of drilling cuttings in different regions. According to the requirements of Chinese standard *Technical specifications on identification for hazardous waste* (HJ/T 298–2019), the sampling quantity is determined according to the total amount of WDC, and the requirements of sample quantity are met.

Testing methods

Detection of organic pollutants in WDC

At present, the determination methods of polycyclic aromatic hydrocarbons in soil mainly include liquid chromatography, gas chromatography mass spectrometry, and other methods. Due to the high sensitivity and strong anti-interference ability of gas chromatography mass spectrometry, it is listed as the designated method of national soil screening. Therefore, this study used Chinese standard *Water quality-Determination of volatile organic compounds-Headspace/Gas chromatography mass spectrometry* (HJ 810–2016) to detect the organic content in WDC.

1. Main experimental instruments

   GC–MS instrument: Agilent 7890B-5977A, with 7693 automatic sampler (Agilent, USA), miVac rotary evaporator (GeneVac, UK), SB-5200DT ultrasonic cleaner, Eppendorf desktop high-speed centrifuge.
2. Instrument condition

   Reference conditions of headspace sampler.

   Heating equilibrium temperature: 65 °C, heating equilibrium time: 40 min, sampling needle temperature: 80 °C, transmission line temperature: 105 °C, sample volume: 1.0 mL.

   GC reference conditions.

   HP-5MS elastic capillary column (30 m × 0.25 mm × 0.25 μm), inlet temperature: 250 °C, carrier gas: helium, sampling mode: split sampling (split ratio 5:1), column flow rate (constant current mode): 1.0 mL/min, the heating program: keeping at 40 °C for 2 min, rising to 120 °C at 5 °C/min for 3 min, then rising to 230 °C at 10 °C/min for 5 min.

   MS reference conditions

   Ion source: electron bombardment (EI) ion source. Ion source temperature: 230 °C. Ionization energy: 70 eV. Interface temperature: 280 °C. Quadrupole temperature: 150 °C. Scanning mode: ion scanning (SIM). Scanning range: 35 ~ 300 amu.
3. Main experimental reagents

   One thousand milligrams per liter standard substances, including benzo(a)anthracene, benzo(k)fluoranthene, benzo(a)pyrene, indeno(1,2,3-cd)pyrene, and dibenzo(a,h)anthracene, Beijing Tanmo Quality Inspection Technology Co., Ltd., all other reagents used are analytically pure.
4. Sample pretreatment and determination

   After preliminary screening, the collected WDC samples were mixed with a certain amount of standard reserve liquid and stirred evenly, and then placed in a grinding brown glass bottle for sealing and avoiding light preservation. The preservation temperature was 4 °C and the shelf life was 10 days.

The 25-g WDC sample was placed in 250-mL glass triangular beaker, adding 40 mL acetonitrile ultrasonic 10 min, standing 15 min, transfer the upper liquid placed in 50-mL plastic centrifuge tube, 5000 r/min centrifugal 5 min, the supernatant after centrifugation through the anhydrous sodium sulfate device, filtration, dehydration, collection of filtrate, circulation 2 times. The filtrate collected twice was concentrated to dryness by rotary evaporator, and 100-μL methanol was added to constant volume. The filtrate was

transferred to the injection bottle with an inner liner for GC/MS analysis.

Human health risk assessment of WDC organic pollutants

The Chinese standard *Technical guidelines for risk assessment of soil contamination of land for construcion* (HJ 25.3–2019) was used for risk assessment and risk control value calculation of organic pollutants in WDC. The calculation formula is as follows:

Calculation of organic matter exposure in WDC

(1) Intake of WDC particles through mouth

The exposure corresponding to the oral intake of solid waste particles is calculated by Formula (1):

$$\mathrm{OISERca} = \frac{\mathrm{OISERca} \times \mathrm{EDa} \times \mathrm{EFa} \times \mathrm{ABSo}}{\mathrm{BWa} \times \mathrm{ATca}} \times 10^{-6} \quad (1)$$

where OISERca is the exposure to oral intake of solid waste particles (carcinogenic effect), kg(soil)•kg^{-1}(body weight)•d^{-1}. Tca is the average time of carcinogenic effect, d; OSIRa is the daily soil intake by adults, mg•d^{-1}. EDa is the adult exposure cycle, a. EFa is the adult exposure frequency, d•a^{-1}. BWa is the larger weight, kg. ABSo is the oral absorption efficiency factor, dimensionless.

(2) Calculation of particle exposure of skin contact WDC

The exposure amount corresponding to the skin contact with WDC particle pathway is calculated by Formula (2):

$$\mathrm{DCSERca} = \frac{\mathrm{SAEa} \times \mathrm{SSARa} \times \mathrm{EFa} \times \mathrm{EDa} \times \mathrm{Ev} \times \mathrm{ABSd}}{\mathrm{BWa} \times \mathrm{ATca}} \times 10^{-6} \quad (2)$$

where DCSERca is the exposure of debris particles in skin contact with WDC (carcinogenic effect), kg(soil)•kg^{-1}(body weight)•d^{-1}. ATca is the average time of carcinogenic effect, d; for other parameters, see Formula (1), and SAEa is the parameter values calculated using Formula (3):

$$\mathrm{SAEa} = 239 \times \mathrm{Ha}^{0.417} \times \mathrm{BWa}^{0.517} \times \mathrm{SEra} \quad (3)$$

where Ha is the average height of adults, cm, and SERa is the adult exposed skin area ratio, dimensionless.

(3) Inhalation of dust particles from WDC by breathing

The amount of soil exposure corresponding to inhalation of soil particulate matter is calculated by Formula (4):

$$\mathrm{PISERca} = \frac{\mathrm{PM10} \times \mathrm{DAIRa} \times \mathrm{EDa} \times \mathrm{PIAF} \times (\mathrm{Fspo} \times \mathrm{EFOa} \times \mathrm{Fspi} \times \mathrm{EFIa})}{\mathrm{BWa} \times \mathrm{ATca}} \times 10^{-6} \quad (4)$$

where PISERca is the soil exposure to inhaled soil particles (carcinogenic effect), kg(soil)•kg^{-1}(body weight)•d^{-1}. PM10 is the inhalable particulate matter content in air, mg•m^{-3}. DAIRa is the daily air respiration of adults, m^3•d^{-1}. PIAF is the inhaled soil particulate matter in vivo retention ratio, dimensionless. Fspi is the proportion of particulate matter from soil in indoor air, dimensionless. Fspo is the proportion of particulate matter from soil in outdoor air, dimensionless. EFIa is the indoor exposure frequency of adults, d•a^{-1}. EFOa is the outdoor exposure frequency of adults, d•a^{-1}. ATca is the average time of carcinogenic effect, d.

(4) Drinking groundwater

The groundwater exposure corresponding to the drinking ground water pathway is calculated by Formula (5):

$$\mathrm{CGWERca} = \frac{\mathrm{CGWERca} \times \mathrm{EFa} \times \mathrm{EDa}}{\mathrm{BWa} \times \mathrm{ATca}} \quad (5)$$

where CGWERca is the exposure to groundwater corresponding to drinking affected groundwater (carcinogenic effect), L(groundwater)•kg^{-1}(body weight)•d^{-1}. ATca is the average time of carcinogenic effect, d.

Calculation of carcinogenic effect of WDC

(a) Oral intake of WDC particles

The carcinogenic risk of single pollutant in the WDC particles is calculated by Formula (6):

$$\mathrm{CR_{oIS}} = \mathrm{OISERca} \times \mathrm{C} \times \mathrm{SFo} \quad (6)$$

where $\mathrm{CR_{ois}}$ is the oral intake of WDC particles exposed to a single pollutant carcinogenic risk, dimensionless. SFo is the oral intake carcinogenic slope factor, (mg•kg^{-1}•d^{-1})$^{-1}$. *C* is the oral intake carcinogenic slope factor, mg•kg^{-1}.

(b) Skin contact with WDC particles

The carcinogenic risk of skin contacting with single pollutant in WDC and particles is calculated by Formula (7):

$$\mathrm{Cr_{DCS}} = \mathrm{DCSER_{ca}} \times \mathrm{C} \times \mathrm{SFd} \quad (7)$$

where $\mathrm{CR_{DCS}}$ is the carcinogenic risk of single pollutant exposure to WDC particles in skin, dimensionless. SFd is the skin contact carcinogenic slope factor, (mg•kg^{-1}•d^{-1})$^{-1}$.

(iii) Respiration inhalation of WDC dust particles

The carcinogenic risk of single pollutant in inhaled dust particles is calculated by Formulas (8) and (9):

$$CR_{PIS} = PISER_{ca} \times C \times SF_i \tag{8}$$

$$SF_i = \frac{IUR \times BW_a}{DAIR_a} \tag{9}$$

where CR_{PIS} is the inhaled dust particles exposed to a single pollutant carcinogenic risk, dimensionless. SFi is the respiratory inhalation carcinogenic slope factor, $(mg \bullet kg^{-1} \bullet d^{-1})^{-1}$. IUR is the unit carcinogenic risk of respiratory inhalation, $m^3 \bullet mg^{-1}$.

(iv) Drinking groundwater

For the risk assessment model of drinking groundwater, according to the actual situation of field investigation, some contents refer to the site pollution risk assessment model of the Chinese standard *Technical guidelines for risk assessment of soil contamination of land for construcion* (HJ 25.3–2019) and RBCA in the USA.

The process of WDC leaching to groundwater can be calculated according to the following Formula (10):

$$LF_{gw} = \frac{\rho_b}{\left(H' \times \theta_{avs} + \theta_{wvs} + K_s + \rho_b\right) \times \left(1 + \frac{U_{gw} \times \delta_{gw}}{I_f \times W_{gw}}\right)} \times \frac{L_1}{L_2} \tag{10}$$

where LF_{gw} is the soil leaching dilution factor, kg/L. U_{gw} is the Darcy rate of groundwater, $cm \bullet a^{-1}$. δ_{gw} is the thickness of groundwater mixed zone, cm. I_f is the net infiltration rate of rainwater, $cm \bullet a^{-1}$. H′ is Henry's constant, dimensionless. θ_{avs} is the volume ratio of pore air in unsaturated soil layer, dimensionless. θ_{wvs} is the volume ratio of pore water in unsaturated soil layer, dimensionless. K_s is the distribution coefficient of pollutants in soil and water $L \bullet kg^{-1}$, organic matter K_s, and inorganic matter $K_s = K_d$. ρ_b is the volume weight of soil, $kg \bullet L^{-1}$. W_{gw} is the length of contaminated area parallel to groundwater flow, cm.

$$K_s = K_{oc} \times f_{oc} \tag{11}$$

$$f_{oc} = \frac{f_{om}}{1.7 \times 1000} \tag{12}$$

where K_{oc} is the distribution coefficient of soil organic carton/soil pore water, $L \bullet kg^{-1}$. f_{oc} is the soil organic carbon mass fraction, dimensionless. f_{om} is the organic matter content, $g \bullet kg^{-1}$.

After rainwater leaches into the bedding area of WDC field, the pollutants are dissolved and enter the groundwater with the leaching solution. The concentration of groundwater pollutants below this area can be calculated according to Formula (13):

$$C_{gw} = LF_{gw} \times C \tag{13}$$

where C_{gw} is the concentrations of pollutants in groundwater, mg/L. LF_{gw} is the soil leaching dilution factor, kg/L. C is concentration of pollutants in WDC, $mg \bullet kg^{-1}$.

The calculation of carcinogenic risk is presented by Formula (14):

$$CR_{cgw} = CGWER_{ca} \times C_{gw} \times SFo \tag{14}$$

where CRcgw is the cancer risk of drinking groundwater, dimensionless. SFo is the oral intake carcinogenic slope factor, $(mg \bullet kg^{-1} \bullet d^{-1})^{-1}$.

Calculation of soil risk control value of heavy metals in WDC

Based on the soil risk control value of carcinogenic effect by oral intake of soil, Formula (15) is used to calculate.

$$RCVS_{ois} = \frac{ACR}{OISER_{ca} \times SF_o} \tag{15}$$

where $RCVS_{ois}$ is the soil risk control value based on carcinogenic effect of oral intake of soil pathway, $mg \bullet kg^{-1}$. $OISER_{ca}$ is the exposure to oral intake of solid waste particles (carcinogenic effect), $kg(soil) \bullet kg^{-1}(body\ weight) \bullet d^{-1}$. ACR is the acceptable carcinogenic risk, dimensionless, value 10^{-5}. SF_o is the oral intake carcinogenic slope factor, $(mg \bullet kg^{-1} \bullet d^{-1})^{-1}$.

Based on the soil risk control value of carcinogenic effect of skin contact with soil, Formula (16) is used to calculate.

$$RCVS_{dcs} = \frac{ACR}{DCSER_{ca} \times SF_d} \tag{16}$$

where $RCVS_{dcs}$ is the soil risk control value based on carcinogenic effect of skin contact with soil pathway, $mg \bullet kg^{-1}$. $DCSER_{ca}$ is the exposure of debris particles in skin contact with WDC (carcinogenic effect), $kg(soil) \bullet kg^{-1}(body\ weight) \bullet d^{-1}$. ACR is the acceptable carcinogenic risk, dimensionless, value 10^{-5}. SF_d is the oral intake carcinogenic slope factor, $(mg \bullet kg^{-1} \bullet d^{-1})^{-1}$.

Based on the soil risk control value of carcinogenic effect by inhalation of soil particles, Formula (17) is used to calculate.

$$RCVS_{pis} = \frac{ACR}{PISER_{ca} \times SF_i} \tag{17}$$

where $RCVS_{dcs}$ is the soil risk control value based on carcinogenic effect of skin contact with soil pathway, $mg \bullet kg^{-1}$. $PISER_{ca}$ is the exposure of inhaled dust particles (carcinogenic effect), $kg(soil) \bullet kg^{-1}(body\ weight) \bullet d^{-1}$. ACR is the acceptable carcinogenic risk, dimensionless, value 10^{-5}. SF_i is the respiratory inhalation carcinogenic slope factor, $(mg \bullet kg^{-1} \bullet d^{-1})^{-1}$.

Based on the soil risk control values of comprehensive carcinogenic effects of three exposure pathways, Formula (18) is calculated according to *Technical guidelines for risk assessment of soil contamination of land for construcion* (HJ 25.3–2019).

$$\mathrm{RCVS_n} = \frac{\mathrm{ACR}}{\mathrm{OISER_{ca}} \times \mathrm{SF_o} \times \mathrm{DCSER_{ca}} \times \mathrm{SF_d} \times \mathrm{PISER_{ca}SF_i}} \quad (18)$$

where $\mathrm{RCVS_n}$ is the soil risk control value of single pollutant (n) based on comprehensive carcinogenic effects of three soil exposure pathways, mg•kg^{-1}.

The radioactive calculation formula of building materials

$$I_{Ra} = C_{Ra}/200 \quad (19)$$

$$I_r = C_{Ra}/370 + C_{Th}/260 + C_K/4200 \quad (20)$$

where C_{Ra}, C_{Th}, and C_{K} are the specific radioactivity (Bq/Kg) of natural radionuclides radium-226, thorium-232, and potassium-40 in building materials, respectively. According to the requirements of Chinese standard *limits of radionuclides in building materials* (GB6566-2010), after testing, when WDC are used as building materials, their I_{Ra} and I_{r} indexes need to be less than or equal to 1.0. According to the *limits of radionuclides in building materials* (GB 6566–2010), the use range of WDC is not limited.

Chemical composition

The chemical analysis of raw materials was distinguished by RIGAKU ZSX Priums up-irradiation X-ray fluorescence spectrometer produced in Japan. The power of X-ray tube is 4 kW.

XRD (X-ray diffraction analysis)

The mineral crystal phase of WDC and its hydrated products were tested by using Netherlands X'Pert Pro XRD, step width is 2 × 0.02°/step, and scanning speed is 80 mm/min.

SEM (scanning electron microscopy)

Microstructure is analyzed with a scanning electron microscope (SEM, ASTEREO SCAN440, Leica Cambridge Ltd) which be used to investigate the morphology and the elemental analysis.

FT-IR (Fourier transform infrared)

The hydration product's chemical bonds of the samples were analyzed by Fourier transform infrared spectroscopy (FT-IR). The readily available for testing powder blended with KBr is then squeezed at 2000 psi for 5 min for analysis; frequency range is 4×10^2, 4×10^3 cm, and 0.5 cm resolution ratio.

Results and discussion

Based on the basic physical and chemical properties of WDC samples, this study comprehensively analyzed the release and migration characteristics of organic pollutants in WDC in various environmental media. The human health and safety risk assessment method was innovatively used to evaluate the safety of organic pollutants in WDC, and the human health and ecological safety risk assessment model was constructed. The pollution control indexes and limits of WDC resource utilization were obtained by calculation. Reasonable control means and resource utilization direction were selected to treat WDC (Loizia et al. 2021a, b), and the safety control mechanism of organic pollutants in resource products was analyzed to comprehensively guarantee the environmental safety and human health of WDC resource products in use.

Risk assessment of organic pollutants in WDC

According to the leaching toxicity test results of WDC in Table 22, all the detected substances do not exceed the limit value in *Identification standards for hazardous wastes-Identification for extraction toxicity* (GB5085.3–2007). The detected heavy metals do not exceed the standard values of residential land in *Risk screening guideline values for soil contamination of development land (three drafts)* (HJ 25.5–2015) and *Soil environmental quality-Risk control standard for soil contamination of agricultural land* (GB 15,618–2018). The detection concentrations of benzo(a) pyrene are all higher than the concentration limit, and the maximum exceeding multiple is 2.37 times, which is the main exceeding factor.

Primary selection of organic pollutants in WDC

WDC were leached by *Water quality-Determination of volatile organic compounds-Headspace /Gas chromatography mass spectrometry* (HJ 810–2016), and WDC of No. A drilling platform, No. B drilling platform, No. C drilling platform, No. D drilling platform, No. E drilling platform, No. F drilling platform, and No. G drilling platform were determined. The test results are shown in Table 1.

Benzo(a)anthracene, benzo(k)fluoranthene, benzo(a) pyrene, indeno(1,2,3-cd)pyrene, and dibenzo(a,h)anthracene exceed the standard values of residential land in *Risk screening guideline values for soil contamination of development land (three drafts)* (HJ 25.5–2015) and *Soil*

Table 1 Organic pollutant content in seven drilling platforms

Item	B platform	A platform	C platform	D platform	E platform	F platform	G platform
Benzo(a)anthracene	0.7256	6.4978	1.4396	0.6987	0.3000	1.8329	0.9730
Benzo(k)fluoranthene	132.4004	3.2343	23.2822	8.6597	15.2000	0.1000	8.7025
Benzo(a)pyrene	0.0765	1.6071	0.1863	0.1000	0.1325	0.1726	0.0935
Indeno(1,2,3-cd)pyrene	1.5204	1.97	1.8300	0.3000	1.0973	0.5469	1.2596
Dibenzo(a,h)anthracene	0.1265	5.9552	0.1637	0.1324	0.1832	0.1754	0.0000

Table 2 Details of main exceeding factors in organic matter

No	Item	Mean value	Minimum value	Maximum value	Number of samples	Standard value	Number of excesses	Exceeding standard rate (%)	Maximum excess multiple (times)
1	Benzo(a) anthracene	1.7811	0.3000	6.4978	7	1.86	1	14.3	3.49
2	Benzo(k) fluoranthene	27.3684	0.1000	132.400	7	18	2	28.6	7.36
3	Benzo(a) pyrene	0.3384	0.1000	1.6071	7	0.19	1	14.3	8.46
4	Indeno(1,2,3-cd)pyrene	1.2177	0.3000	1.9752	7	1.87	1	14.3	1.06
5	Dibenzo(a,h) anthracene	0.9623	0.0000	5.9552	7	0.19	1	14.3	31.34

environmental quality-Risk control standard for soil contamination of agricultural land (GB 15,618–2018). The maximum exceeding multiples of residential land standards exceeding *Risk screening guideline values for soil contamination of development land (three drafts)* (HJ 25.5–2015) are 3.49, 7.36, 8.46, 1.06, and 31.34 times, respectively. And benzo(a)pyrene also exceeds *Soil environmental quality-Risk control standard for soil contamination of agricultural land* (GB 15,618–2018); the maximum exceeding multiple is 15.07 times. Other indicators do not exceed the corresponding standards, so benzo(a)anthracene, benzo(k) fluoranthene, benzo(a)pyrene, indeno(1,2,3-cd)pyrene, and dibenzo(a,h)anthracene are the main exceeding factors, and the specific exceeding conditions are shown in Table 20 in Annex 2. Therefore, benzo(a)anthracene, benzo(a)pyrene, indeno(1,2,3-cd)pyrene, and dibenzo(a,h)anthracene in the solid phase of WDC are the main control factors (Wang et al. 2018a, b, c, d; Rehman et al. 2017). The leaching results of organic pollutants and the main exceeding factors are shown in Table 2.

Risk control calculation of comprehensive utilization index of WDC

The solid phase of WDC is used to lay the foundation materials of the non-sensitive regional open well road and bedding well site. In order to ensure the human health of the site, it is necessary to carry out the risk assessment and determine the risk control value of the site soil. Therefore, the Chinese standard *Technical guidelines for risk assessment of soil contamination of land for construcion* (HJ 25.3–2019) is used for risk assessment and risk control value calculation of organic pollutants in WDC. The whole assessment process mainly includes hazard identification, toxicity assessment, exposure assessment, risk representation, and control value calculation (Boulicault et al. 2016; Tsangas et al. 2019).

Hazard identification When the solid phase comprehensive utilization of WDC generated during shale gas development is set to be used for bedding and road construction in the well site, the comprehensive utilization area is located around the drilling platforms in Chongqing area, belonging to industrial land, so the possible sensitive receptors are mainly human body and soil (Davarpanah et al. 2018).

Toxicity assessment On the basis of hazard identification, this study considered the impact of pollutants in WDC on human health through various migration pathways after cushion utilization and road construction in the region. Specific content of solid waste toxicity assessment includes analysis of health effects (including carcinogenic and non-carcinogenic effects) and determination of toxic parameter values of pollutants. The toxicity parameters used in this study are shown in Table 21 in Annex 2. The toxicity

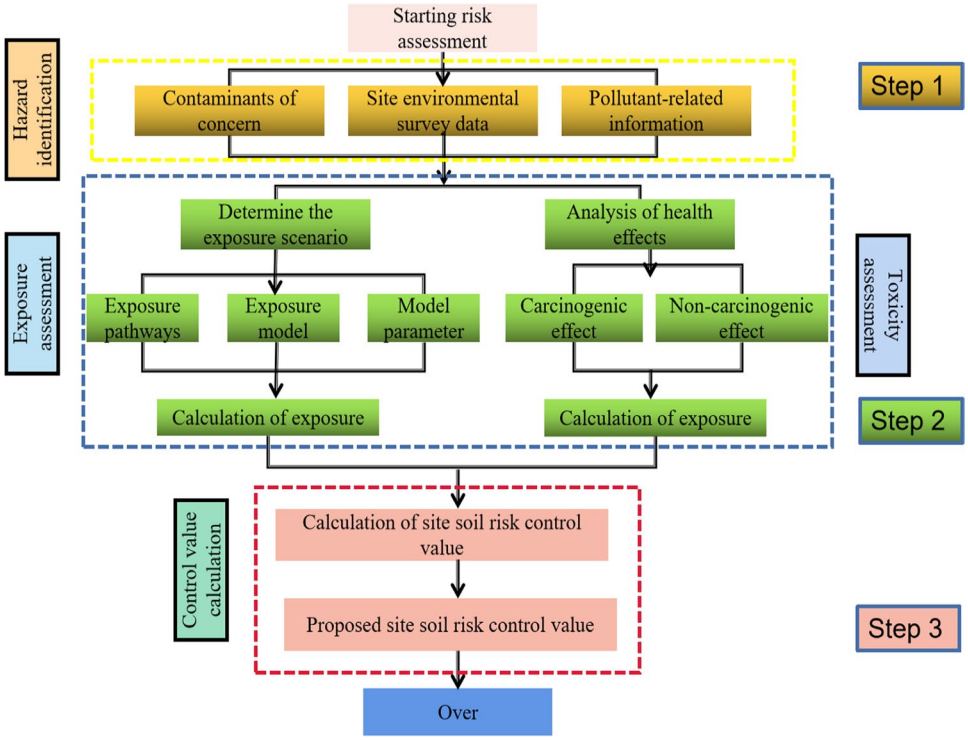

Fig. 1 Risk assessment procedures and contents of pollutant sites

parameters are derived from the database of RBCA site risk assessment software and the data collation of solids from the Chinese Academy of Environmental Sciences.

Exposure assessment Exposure assessment is to use the model to predict the migration and transformation process of pollutants from source to medium, and analyze the spatial distribution and release concentration of pollutants related to the evaluation area. That is to say, the process of measurement, estimation or prediction of exposure amount, exposure frequency, exposure duration, and exposure pathway under the condition of target harmful pollutants or physical factors is the quantitative basis for risk assessment (Mojoudi et al. 2019). Overall, exposure assessment includes three aspects: analysis of exposure scenarios, determination of exposure pathways, and exposure calculation (Fig. 1).

a. Analysis of exposure scenarios

WDC are used as well site bedding area to plan drilling platforms (industrial land) in Chongqing area. Combined with field survey results, the following evaluation exposure scenarios are established. Due to the existence of sensitive people in the park, considering the influence of well site bedding on this part of the sensitive population, the standard well site of 4 wells/platform is selected as the scene of this risk assessment.

b. Determination of exposure pathways

Exposure pathways are closely related to pollution sources, location, environmental release types, population location, and activity patterns, including four elements: sources and chemical release mechanisms, retention or transport media (or chemical transport media), exposure pathways of potential populations to pollution media, and contact points. According to the analysis of exposure pathways in this study, the exposure pathways of pollutants to human body include skin absorption, respiratory system inhalation, and digestive system intake (Salari et al. 2019). The exposure pathway analysis and schematic diagram of WDC pollutants are shown in Table 3, respectively. The specific exposure pathways can be refined as follows: (1) platform workers inadvertently intake solid waste particles at work; (2) the skin of platform workers exposed to solid waste particles at work; (3) platform workers breathe in solid waste dust particles; (4) platform workers directly drink groundwater below the area.

iii. Calculation of exposure

Exposure parameters include exposure frequency, exposure period, intake of pollutants, and related parameters of human body. According to the field investigation results and related data of shale gas field operation area, the exposure parameters are selected with reference to the *Technical*

Table 3 Analysis of exposure pathways of pollutants for bedding utilization in WDC field

Exposure scenario	Target pollutant	Exposure pathways	Receptor
WDC well site bedding utilization	Benzo(a)anthracene, benzo(k)fluoranthene, benzo(a) pyrene, dibenzo(a, h)anthracene	Intake of WDC particles through mouth	Worker
		Skin contact with WDC particles	
		Inhalation of dust particles from cuttings in WDC by breathing	
		Groundwater in drinking pad area	

Table 4 Calculation results of oral intake of WDC particles

Parameter name		Unit	Parameter value	Source of parameters
OSIRa	Daily soil intake by adults	$mg{\cdot}d^{-1}$	100.00	Guidelines for risk assessment
EDa	Adult exposure cycle	a	25.00	Guidelines for risk assessment
EFa	Adult exposure frequency	$d{\cdot}a^{-1}$	250.00	Guidelines for risk assessment
BWa	Larger weight	kg	56.80	Guidelines for risk assessment
ABSo	Oral intake absorption efficiency factor	Zero dimension	1.00	Guidelines for risk assessment
ATca	Average time of carcinogenic effect	d	26,280.00	Guidelines for risk assessment
OISERca	The exposure amount of WDC particles taken orally (carcinogenic effect)	$kg{\bullet}kg^{-1}{\bullet}d^{-1}$	4.19E-07	Computation

guidelines for risk assessment of soil contamination of land for construcion (HJ 25.3–2019) and RBCA site risk assessment software (Fu et al. 2019; Issabayeva et al. 2018). Some of the data are estimated according to the actual situation of the site. At the same time, in the selection of exposure parameters, we consider the principle of limited adverse conditions hypothesis, and evaluate the potential harm to the human body and the surrounding environment under the adverse conditions. The specific parameters are shown in Table 22 in Annex 2. Because PAHs are carcinogenic pollutants, we only need to consider the carcinogenic effect exposure of a single pollutant.

Reselection of organic pollutants from WDC

Calculation of organic matter exposure in WDC The main pollutants concerned in the evaluation of WDC/mud are five polycyclic aromatic hydrocarbons (PAHs), namely, anthracene, benzo(k)fluoranthene, benzo(a)pyrene, dibenzo(a,h) anthracene, and indeno(1,2,3-cd)pyrene. The toxicity parameters of major PAHs are shown in Table 21 in Annex 2. In the scenario of WDC well site bedding and other utilization, it is concerned that pollutants are carcinogenic substances. In the domestic wind assessment guidelines, there are corresponding ways of carcinogenic risk slope factor parameters, so only the carcinogenic risk of each pollutant is calculated. In the calculation, the maximum average concentration is used as the pollution source concentration for risk assessment, that is, the overall risk level is estimated in a relatively conservative way (Okparanma et al. 2018).

i) Intake of WDC particles through mouth

For the carcinogenic effect of a single pollutant, consider the lifetime hazards of exposure in adults. The calculation formula is shown in Formula (1). The calculation results of exposure amount of WDC through mouth are shown in Table 4. It can be seen from the table that the exposure amount (carcinogenic effect) of WDC taken orally is 4.19×10^{-7} $kg{\bullet}kg^{-1}{\bullet}d^{-1}$.

ii) Calculation of particle exposure of skin contact WDC

For the carcinogenic effect of single pollutant, consider the lifelong hazard of human exposure in adulthood. The calculation formula is shown in Formula (2). The calculation results of debris particle exposure in skin contact WDC are shown in Table 5. It can be seen from the table that the exposure amount (carcinogenic effect) of skin contacting WDC particles is 3.11×10^{-7} $kg{\bullet}kg^{-1}{\bullet}d^{-1}$.

iii) Inhalation of dust particles from WDC by breathing

In industrial and other land use, humans can breathe in indoor and outdoor air from soil particles exposed to soil pollutants. For carcinogenic effects of single pollutants, the lifetime hazards of exposure in adults are considered. The calculation formula is shown in Formula (4). The calculation results of dust particles from WDC by breathing are shown in Table 6. It can be seen from the table that the

Table 5 Calculation results of exposure to WDC particles in skin contact

Parameter name		Unit	Parameter value	Source of parameters
Ha	Average height of adults	cm	156.30	Guidelines for risk assessment
SERa	Adult exposed skin area ratio	Zero dimension	0.18	Guidelines for risk assessment
SAEa	Adult exposed skin surface area	cm^2	2854.63	Computation
SSARa	Soil adhesion coefficient of adult skin surface	$mg{\cdot}cm^{-2}$	0.20	Guidelines for risk assessment
ABSd	Skin contact absorption efficiency factor	Zero dimension	0.13	RBCA Site Risk Assessment Software
Ev	Daily frequency of skin contact events	$meta{\cdot}d^{-1}$	1.00	Guidelines for risk assessment
EFa	Adult exposure frequency	$d{\cdot}a^{-1}$	250.00	Guidelines for risk assessment
EDa	Adult exposure cycle	a	25.00	Guidelines for risk assessment
BWa	Larger weight	kg	56.80	Guidelines for risk assessment
ATca	Average time of carcinogenic effect	d	26,280.00	Guidelines for risk assessment
DCSERca	Exposure of skin to WDC and oil-based ash particles (carcinogenic effect)	$kg{\bullet}kg^{-1}{\bullet}d^{-2}$	3.11E-07	Computation

Table 6 Calculation of soil exposure to respiratory inhalation

Parameter name		Unit	Parameter value	Source of parameters
PM10	Inhalable particulate matter content in air	$mg{\cdot}m^{-3}$	0.15	Guidelines for risk assessment
DAIRa	Daily air respiration of adults	$m^3{\cdot}d^{-1}$	14.5	Guidelines for risk assessment
PIAF	The retention ratio of inhaled soil particles in the body	Zero dimension	0.75	Guidelines for risk assessment
Fspi	Proportion of particulate matter from soil in indoor air	Zero dimension	0.8	Guidelines for risk assessment
Fspo	Proportion of particulate matter from soil in outdoor air	Zero dimension	0.5	Guidelines for risk assessment
EFIa	Indoor exposure frequency of adults	$d{\cdot}a^{-1}$	187.5	Guidelines for risk assessment
EFOa	Outdoor exposure frequency of adults	$d{\cdot}a^{-1}$	62.5	Guidelines for risk assessment
EDa	Adult exposure cycle	a	25	Guidelines for risk assessment
BWa	Larger weight	kg	56.8	Guidelines for risk assessment
ATca	Average time of carcinogenic effect	d	26,280	Guidelines for risk assessment
PISERca	Inhaled soil particle exposure (carcinogenic)	$kg{\cdot}kg^{-1}{\cdot}d^{-1}$	4.95E-09	Computation

Table 7 Calculation results of exposure of drinking groundwater

Parameter name		Unit	Parameter value	Source of parameters
GWCRa	Daily water intake for adults	$L{\bullet}d^{-1}$	1.00	Guidelines for risk assessment
EDa	Adult exposure cycle	a	25.00	Guidelines for risk assessment
EFa	Adult exposure frequency	$d{\cdot}a^{-1}$	250.00	Guidelines for risk assessment
BWa	Larger weight	kg	56.80	Guidelines for risk assessment
ATca	Average time of carcinogenic effect	d	26,280.00	Guidelines for risk assessment
CGWERca	Exposure of drinking groundwater (carcinogenic effect)	$L{\bullet}kg^{-1}{\bullet}d^{-1}$	4.19E-03	Computation

exposure amount (carcinogenic effect) of inhaled WDC is 4.95×10^{-6} $kg{\bullet}kg^{-1}{\bullet}d^{-1}$.

iv) Drinking groundwater

For the carcinogenic effect of a single pollutant, consider the exposure hazards of the population in adulthood. The calculation formula is shown in Formula (5). The calculation results of exposure of drinking groundwater are shown in Table 7. The table shows that the exposure (carcinogenic effect) of drinking groundwater is 4.19×10^{-3} $L{\bullet}kg^{-1}{\bullet}d^{-1}$.

Calculation of carcinogenic effect of WDC.

The main pollutants in the evaluation of WDC mud are benzo(a)anthracene, benzo(k)fluoranthene, benzo(a)pyrene, dibenzo(a,h)anthracene, and indeno(1,2,3-cd)

Table 8 Risk calculation results of WDC particles intake by mouth

Parameter name			Unit	Parameter value	Source
OISERca	Oral exposure to WDC particles (carcinogenic effect)		$kg•kg^{-1}•d^{-1}$	4.19E-07	Computation
C	WDC	Benzo(a)anthracene	$mg•kg^{-1}$	3.3989	Average maximum concentration
		Benzo(k)fluoranthene	$mg•kg^{-1}$	66.2500	Average maximum concentration
		Benzo(a)pyrene	$mg•kg^{-1}$	0.9536	Average maximum concentration
		Dibenzo(a,h)anthracene	$mg•kg^{-1}$	5.9552	Average maximum concentration
		Indeno(1,2,3-cd)pyrene	$mg•kg^{-1}$	1.1376	Average maximum concentration
SFo	Oral intake carcinogenic slope factor	Benzo(a)anthracene	$(mg•kg^{-1}•d^{-1})^{-1}$	7.30E-01	Guidelines for risk assessment
		Benzo(k)fluoranthene	$(mg•kg^{-1}•d^{-1})^{-1}$	7.30E-02	Guidelines for risk assessment
		Benzo(a)pyrene	$(mg•kg^{-1}•d^{-1})^{-1}$	7.30E+00	Guidelines for risk assessment
		Dibenzo(a,h)anthracene	$(mg•kg^{-1}•d^{-1})^{-1}$	7.30E+00	Guidelines for risk assessment
		Indeno(1,2,3-cd)pyrene	$(mg•kg^{-1}•d^{-1})^{-1}$	7.30E-01	Guidelines for risk assessment
SAF	Reference dose distribution coefficient exposed to soil		Zero dimension	0.20	Guidelines for risk assessment
CR_{OIS}	Oral intake of WDC particles exposed to single pollutant carcinogenic risk	Benzo(a)anthracene	Zero dimension	1.04E-06	Computation
		Benzo(k)fluoranthene	Zero dimension	2.03E-06	Computation
		Benzo(a)pyrene	Zero dimension	2.92E-06	Computation
		Dibenzo(a,h)anthracene	Zero dimension	1.82E-05	Computation
		Indeno(1,2,3-cd)pyrene	Zero dimension	3.48E-07	Computation

pyrene. The toxicity parameters of major PAHs are shown in Table 21 in Annex 2. Referring to the Chinese standard of *Soil environmental quality-Risk control standard for soil contamination of agricultural land* (GB 15,618–2018), in the scenario of WDC well site bedding and other utilization, it is concerned that pollutants are carcinogenic substances. In the domestic wind assessment, there are corresponding carcinogenic risk slope factor parameters, so only the carcinogenic risk of each pollutant is calculated. In the calculation, the maximum average concentration is used as the pollution source concentration for risk assessment, that is, the overall risk level is estimated in a relatively conservative way (Elmouwahidi et al. 2017).

(1) Oral intake of WDC particles

The calculating carcinogenic effects of oral WDC granules are presented in Formula (6). The risk calculation results of WDC intake through mouth are shown in Table 8.

(2) Skin contact with WDC particles

The carcinogenic effect of skin contact with WDC particles is presented in Formula (7). The risk calculation results of skin contact with WDC particles are shown in Table 9.

(3) Respiration inhalation of WDC dust particles

The carcinogenic effect of breathing inhaled WDC dust particles is presented in Formulas (8) and (9). The risk calculation results of inhalation of WDC and dust particles are shown in Table 10.

(4) Drinking groundwater

WDC are leached and soaked by rainwater after bedding utilization. The pollutants in WDC dissolve with rainwater and diffuse into groundwater with the migration and diffusion of leaching solution (Voukali et al. 2021; Sean et al. 2021). The schematic diagram of leaching process is shown in Fig. 2.

In this study, according to the actual situation of field investigation, some contents refer to the site pollution risk assessment model of the Chinese standard *Technical guidelines for risk assessment of soil contamination of land for construcion* (HJ 25.3–2019) and RBCA in the USA. The process of WDC leaching to groundwater can be calculated according to Formula (10). The calculation results of leaching dilution factor LF_{gw} in the bedding utilization process of WDC field are shown in Table 17 in Annex 1.

After rainwater leaches into the bedding area of WDC field, the pollutants are dissolved and enter the groundwater with the leaching solution. The concentration of groundwater pollutants below this area can be calculated according to Formula (13). The calculation of carcinogenic risk is

Table 9 Risk calculation results of skin contact with WDC particles

Parameter name			Unit	Parameter value	Source of parameters
DCSERca	Exposure of skin to WDC particles (carcinogenic effect)		$kg•kg^{-1}•d^{-1}$	3.11E-07	Computation
C	WDC pollutant concentration	Benzo(a)anthracene	$mg•kg^{-1}$	3.3989	Average maximum concentration
		Benzo(k)fluoranthene	$mg•kg^{-1}$	66.2500	Average maximum concentration
		Benzo(a)pyrene	$mg•kg^{-1}$	0.9536	Average maximum concentration
		Dibenzo(a,h)anthracene	$mg•kg^{-1}$	5.9552	Average maximum concentration
		Indeno(1,2,3-cd)pyrene	$mg•kg^{-1}$	1.1376	Average maximum concentration
SF_d	Skin contact carcinogenic slope factor	Benzo(a)anthracene	$(mg•kg^{-1}•d^{-1})^{-1}$	7.30E-01	Guidelines for risk assessment
		Benzo(k)fluoranthene	$(mg•kg^{-1}•d^{-1})^{-1}$	7.30E-02	Guidelines for risk assessment
		Benzo(a)pyrene	$(mg•kg^{-1}•d^{-1})^{-1}$	7.30E+00	Guidelines for risk assessment
		Dibenzo(a,h)anthracene	$(mg•kg^{-1}•d^{-1})^{-1}$	7.30E+00	Guidelines for risk assessment
		Indeno(1,2,3-cd)pyrene	$(mg•kg^{-1}•d^{-1})^{-1}$	7.30E-01	Guidelines for risk assessment
SAF	Reference dose distribution coefficient exposed to soil		Zero dimension	0.20	Guidelines for risk assessment
CR_{OIS}	Exposure of skin contact with WDC particles to single pollutant carcinogenic risk	Benzo(a)anthracene	Zero dimension	7.72E-07	Computation
		Benzo(k)fluoranthene	Zero dimension	1.51E-06	Computation
		Benzo(a)pyrene	Zero dimension	2.16E-06	Computation
		Dibenzo(a,h)anthracene	Zero dimension	1.35E-05	Computation
		Indeno(1,2,3-cd)pyrene	Zero dimension	2.58E-07	Computation

presented by Formula (14). The risk calculation results of drinking groundwater in WDC field are shown in Table 18 in Annex 1.

Through the risk calculation, it can be seen that the cumulative carcinogenic risk of organic matter in the bedding utilization process of WDC well site is shown in Table 11. It can be seen that the cumulative carcinogenic risk of dibenzo(a,h) anthracene reaches 3.17E-05, which exceeds that of Chongqing in *Technical guidelines for risk assessment of soil contamination of land for construcion* (HJ 25.3–2019). The acceptable risk level of contaminated site is the cumulative carcinogenic risk value of 10^{-5}, so it is not acceptable.

Through the above environmental risk calculation, the following conclusions can be drawn, in view of the carcinogenic risk: the cumulative carcinogenic risk of particle intake and skin contact pathway is at an unacceptable level, but the risk level of particle intake and skin contact is relatively low, and the corresponding environmental risk can be controlled by certain preventive measures, and the cumulative carcinogenic risk of dust inhalation and drinking groundwater is at an acceptable level. The comprehensive carcinogenic risk of all exposure pathways of single pollutant benzo(a)anthracene, benzo(a)pyrene, benzo(k)fluoranthene, and indeno(1,2,3-cd)pyrene is acceptable. The cumulative carcinogenic risks of particle intake of dibenzo(a,h) anthracene and skin contact pathway are at an unacceptable level.

Therefore, in view of the carcinogenic risk of dibenzo(a,h)anthracene, the soil limit calculation results of the comprehensive carcinogenic risk of all exposure pathways are shown in Table 11. According to the most unfavorable principle, the exposure amount of inhaled dust particles is calculated by the exposure amount (maximum) at 100 m downwind of oil-based ash (Demetriou et al. 2021).

Calculation of soil risk control value of organic matter in WDC The calculation results of soil risk control values based on carcinogenic effects under different exposure conditions are shown in Table 19 in Annex 1.

Based on the combined carcinogenic effects of three exposure pathways, the soil risk control values were calculated by Formula (18). The detailed calculation process is shown in Table 12.

Based on the soil limits of carcinogenic risk calculated by Formula (18), the recommended control value of pollutant concentration is selected.

According to the risk assessment results shown in Table 13, the dibenzo(a,h)anthracene in WDC is required to be less than 1.8700 mg/kg under the environment of laying open well path and bedding well site with WDC.

Actual resource utilization process of WDC

Macroscopic analysis of WDC road cushion

The contents of toxic substances in WDC collected from A and B drilling platforms are analyzed, and the results are shown in Table 20 in Annex 2. Figure 3 shows the experimental results of WDC samples with different cement contents soaked for 28 days and 128 days respectively. The

Table 10 Risk calculation results for inhalation of WDC dust particles

Parameter name				Unit	Parameter value	Source of parameters
PISERca	Exposure of inhaled dust particles (carcinogenic effect)			$kg \bullet kg^{-1} \bullet d^{-1}$	4.95E-09	Computation
C	WDC pollutant concentration	Benzo(a)anthracene		$mg \bullet kg^{-1}$	3.3989	Average maximum concentration
		Benzo(k)fluoranthene		$mg \bullet kg^{-1}$	66.2500	Average maximum concentration
		Benzo(a)pyrene		$mg \bullet kg^{-1}$	0.9536	Average maximum concentration
		Dibenzo(a,h)anthracene		$mg \bullet kg^{-1}$	5.9552	Average maximum concentration
		Indeno(1,2,3-cd)pyrene		$mg \bullet kg^{-1}$	1.1376	Average maximum concentration
IUR	Unit carcinogenic risk of respiratory inhalation	Benzo(a)anthracene		$(mg/m^3)^{-1}$	1.10E-01	Guidelines for risk assessment
		Benzo(k)fluoranthene		$(mg/m^3)^{-1}$	1.10E-01	Guidelines for risk assessment
		Benzo(a)pyrene		$(mg/m^3)^{-1}$	1.10E + 00	Guidelines for risk assessment
		Dibenzo(a,h)anthracene		$(mg/m^3)^{-1}$	1.20E + 00	Guidelines for risk assessment
		Indeno(1,2,3-cd)pyrene		$(mg/m^3)^{-1}$	1.10E-01	Guidelines for risk assessment
SFi	Respiratory inhalation carcinogenic slope factor	Benzo(a)anthracene		$(mg \bullet kg^{-1} \bullet d^{-1})^{-1}$	4.30E-01	Guidelines for risk assessment
		Benzo(k)fluoranthene		$(mg \bullet kg^{-1} \bullet d^{-1})^{-1}$	4.30E-01	Guidelines for risk assessment
		Benzo(a)pyrene		$(mg \bullet kg^{-1} \bullet d^{-1})^{-1}$	4.30E + 00	Guidelines for risk assessment
		Dibenzo(a,h)anthracene		$(mg \bullet kg^{-1} \bullet d^{-1})^{-1}$	4.70E + 00	Guidelines for risk assessment
		Indeno(1,2,3-cd) pyrene		$(mg \bullet kg^{-1} \bullet d^{-1})^{-1}$	4.30E-01	Guidelines for risk assessment
CR_{PIS}	Exposure of inhalation dust particles to single pollutant carcinogenic risk	WDC	Benzo(a)anthracene	Zero dimension	7.23E-09	Computation
			Benzo(k)fluoranthene	Zero dimension	1.41E-07	Computation
			Benzo(a)pyrene	Zero dimension	2.03E-08	Computation
			Dibenzo(a,h)anthracene	Zero dimension	1.39E-07	Computation
			Indeno(1,2,3-cd) pyrene	Zero dimension	2.42E-09	Computation

experimental results show that the color of water bubbles of WDC samples with different cement contents is different under the same soaking days in water. At the same time, the water bubbles of WDC samples soaked for 128 days are still clear and there is no obvious leaching of pollutants, indicating that the WDC samples are safe after treatment (Antoniou and Antoniou 2019; Wang et al. 2018a, b, c, d).

The 7-day unconfined compressive strength of WDC specimens with different cement contents is shown in Fig. 4. Obviously, when the cement content is 6%, the unconfined compressive strength of 7 days reaches 3.1 MPa, which meets the requirements of the Chinese standard *Technical Guidelines for Construction of Highway Roadbases* (JTG/T F20-2015). When the content is 8%, the strength of the specimen decreases. This is because the C-S–H gel generated by cement hydration in the cementitious reaction wrapped WDC particles, which hindered the hydration of WDC particles and reduced the strength of the specimen. When the cement content was 10%, more C-S–H gels and AFt crystals were produced by cement hydration, which increased the strength of the specimen. Therefore, when the cement content is 10% and 12%, the strength of the specimen is higher. However, the cement content of 6% has met the standard requirements, in order to reduce the economic cost of construction and reduce carbon emissions. Therefore, when WDC are used

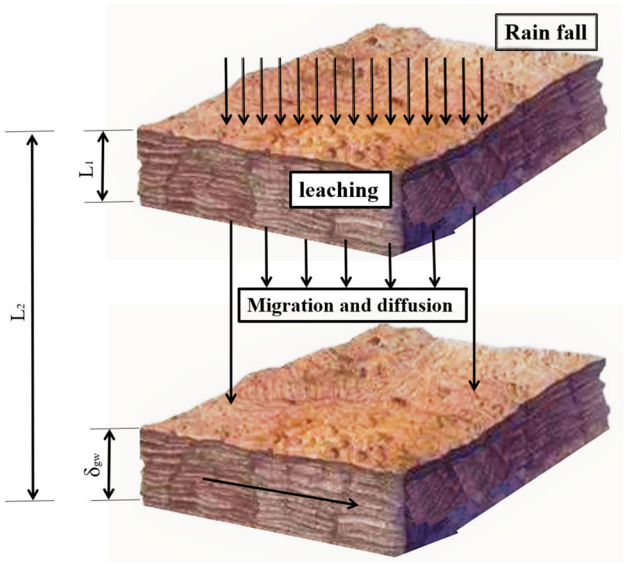

Fig. 2 Groundwater exposure pathway diagram of WDC well site during bedding utilization

as road cushion, the selected cement mass is 6%. Preliminary trial with WDC for road cushion specific formula is as follows: visible WDC content of 50% of the 7-day unconfined compressive strength of 3.1 MPa, if continue to increase the dosage of its early compressive strength, qualification rate is difficult to guarantee, so the maximum dosage of 50%.

As shown in Table 14, the 7-day unconfined compressive strength of the cushion with 50% WDC basically meets the design requirements. So when designing road cushion, the cement content in the formula should not be more than 8% and WDC content should not be higher than 50% by using 42.5 ordinary Portland cement supplemented by part of the debris and water-mixed particles of WDC (Ayati et al. 2019; Senneca et al. 2020). In the construction process, 20 t and above static pressure rollers should be used, and the final well site cushion compaction degree should not be less than 93%, and the 7-day unconfined compressive strength should not be less than 3.0 MPa.

Table 11 Cumulative carcinogenic risk of organic matter during bedding utilization in WDC field

Contaminant		Cancer risk by exposure pathways				Carcinogenic risk of all exposure pathways of single pollutant
		Oral intake of solid waste particles	Skin Contact Solid Waste Particles	Inhaled dust particles	Drinking groundwater	
WDC	Benzo(a)anthracene	1.04E-06	7.72E-07	7.23E-09	2.53E-08	1.84E-06
	Benzo(k)fluoranthene	2.03E-06	1.51E-06	1.41E-07	1.49E-08	3.70E-06
	Benzo(a)pyrene	2.92E-06	2.16E-06	2.03E-08	2.14E-08	5.12E-06
	Dibenzo(a,h)anthracene	1.82E-05	1.35E-05	1.39E-07	4.10E-08	3.19E-05
	Indeno(1,2,3-cd)pyrene	3.48E-07	2.58E-07	2.42E-09	4.31E-10	6.09E-07

Table 12 Calculation of soil limits based on comprehensive carcinogenic risk of all exposure pathways

Parameter name			Unit	Parameter value	Source of parameters
$OISER_{ca}$	The exposure amount of water-based drilling cuttings particles taken orally (carcinogenic effect)		$kg \bullet kg^{-1} \bullet d^{-1}$	4.19E-07	Computation
SFo	Oral intake carcinogenic slope factor	Dibenzo(a,h)anthracene	$(mg \bullet kg^{-1} \bullet d^{-1})^{-1}$	7.30E + 00	Computation
$DCSER_{ca}$	Exposure of skin to water-based drilling cuttings particles (carcinogenic effect)		$kg \bullet kg^{-1} \bullet d^{-2}$	3.11E-07	Computation
SF_d	Skin contact carcinogenic slope factor	Dibenzo(a,h)anthracene	$(mg \bullet kg^{-1} \bullet d^{-1})^{-1}$	7.30E + 00	Computation
$PISER_{ca}$	Exposure of inhaled dust particles (carcinogenic effect)		$kg \bullet kg^{-1} \bullet d^{-1}$	4.95E-09	Computation
SF_i	Respiratory inhalation carcinogenic slope factor	Dibenzo(a,h)anthracene	$(mg \bullet kg^{-1} \bullet d^{-1})^{-1}$	4.70E + 00	Computation
ACR	Acceptable hazard value		Zero dimension	10^{-5}	Chongqing area
$RCVS_n$	Soil limits for carcinogenic risk based on all exposure pathways	Dibenzo(a,h)anthracene	$mg \bullet kg^{-1}$	1.8700	Computation

Table 13 Control target values calculated by all approaches

Calculus process	Calculation results of target value (mg/kg) Dibenzo(a,h)anthracene
Soil limit for carcinogenic risk (acceptable risk 10^{-5})	1.8700

the samples with different cement ratios. The results show that the infrared spectrum curves of the samples with cement ratios of 6%, 8%, 10%, and 12% are roughly the same, indicating that the hydration products of the WDC samples do not change significantly at the early and late stages of hydration (Wang et al. 2019). The results show that the infrared absorption peak at 1034.8 cm^{-1} is the corresponding of the symmetric and asymmetric stretch-

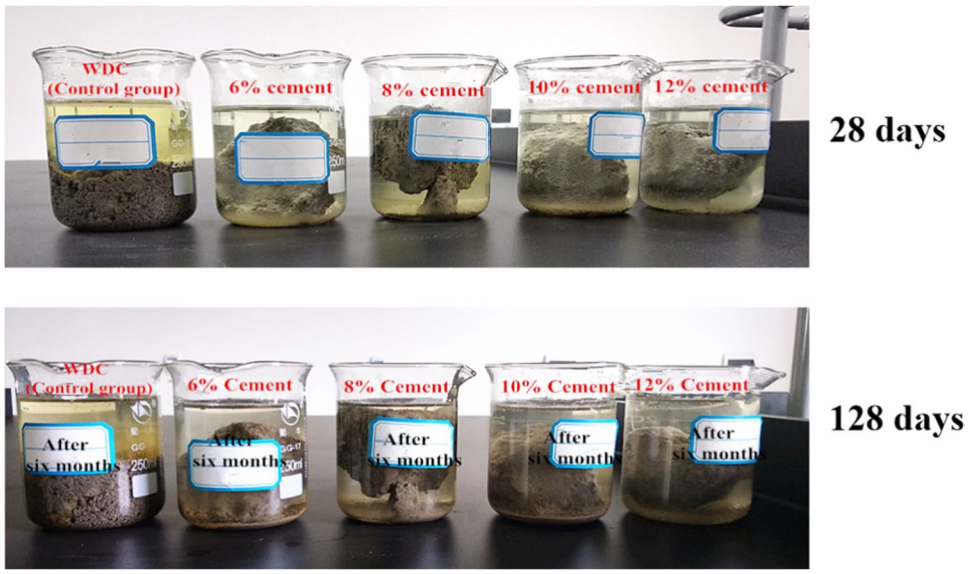

Fig. 3 WDC samples with different cement ratios

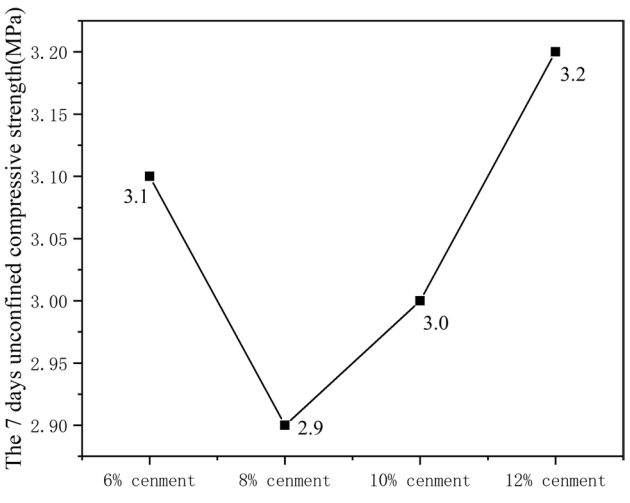

Fig. 4 Effect of different cement contents on the strength of WDC-cement system

Table 14 WDC road cushion mix proportion

No	Cement (%)	WDC (%)	Crushed stone (%)	Water (%)	The 7-day unconfined compressive strength (MPa)
1 (50%)	6	50	44	Proper	3.1

Microscopic analysis of WDC road cushion

Fourier transform infrared (FT-IR) can give the hint of bending vibration and stretching of Al-O and Si–O whose vibration frequencies increase with the increase of polymerization degree. Figure 5 shows the infrared spectrum of

ing vibration of sulfate in $CaSO_4$. The absorption peak of 3442.9 cm^{-1} corresponds to the bending and stretching vibrations of H–O in $Ca(OH)_2$. The characteristic absorption peaks of ettringite and calcium aluminate hydrate are 1112.0 cm^{-1} and 1419.7 cm^{-1}, respectively. The absorption peak intensity of AFt and calcium aluminate hydrate increased slightly with the increase of cement content from 6 to 10%. If the cement content exceeds 10%, they will fall sharply. In addition, the absorption peak intensity of $Ca(OH)_2$ decreases with the increase of WDC content. It is directly proved that the volcanic ash activity of WDC is caused by the active reaction of CaO with SiO_2 and the active reaction of gypsum and CaO with Al_2O_3 to form ettringite (Han et al. 2020; Hossain et al. 2020).

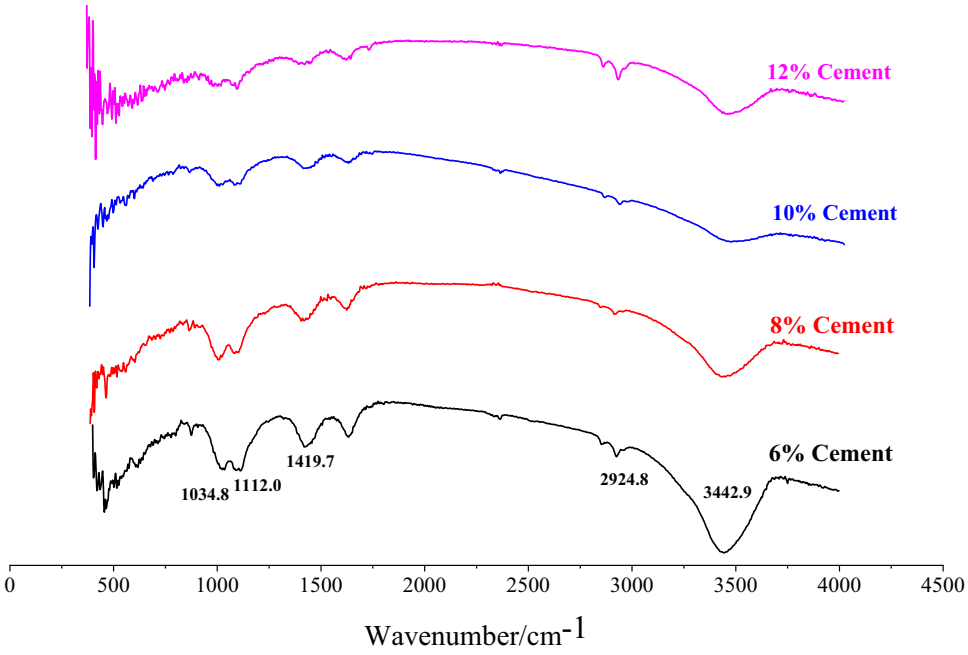

Fig. 5 FT-IR spectrums of WDC with different cement ratios

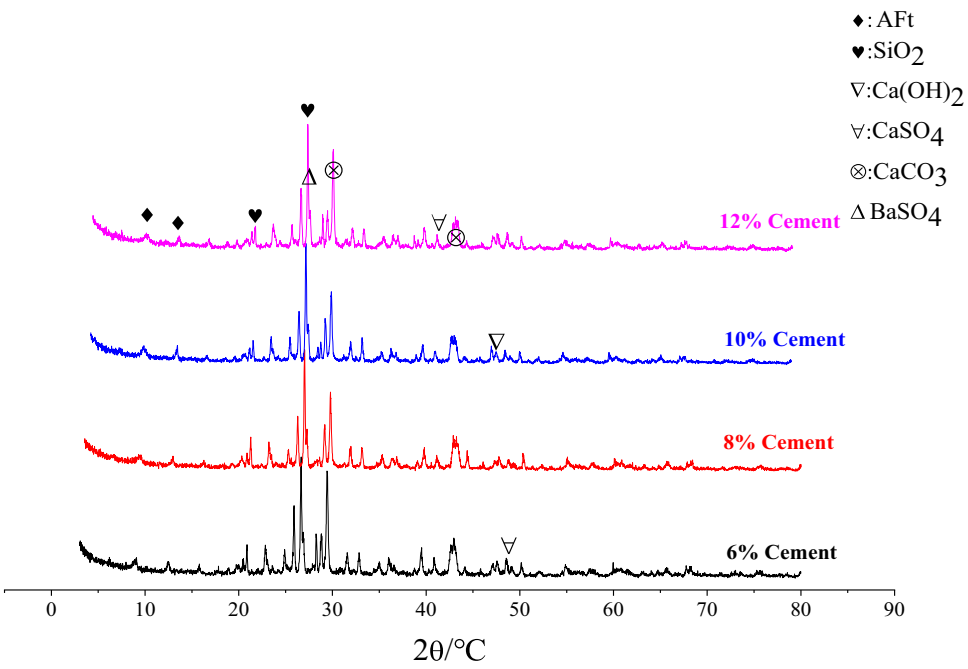

Fig. 6 WDC samples with different cement ratios and XRD patterns

Based on the curing principle of ettringite and C-S–H colloid generated during cement hydration on organic pollutants in WDC, in order to further study the role of WDC in road buffer system, cement with different contents is mixed with WDC and fine aggregate, and the hydration products of the system were studied by WDC (Senneca et al. 2020; Foroutan et al. 2018). The results show that the main crystalline phases identified in the hardened slurry of road cushion are ettringite, quartz, $CaCO_3$, $Ca(OH)_2$, and $CaSO_4$. As shown in Fig. 6, with the addition of WDC, the crystal phase difference in XRD is large, and the intensity of diffraction peak at 47.8 is significantly reduced or even disappeared, indicating that there were more hydration products generated in the hydration process of WDC dissolved active alumina and silicate cement (Hossain et al. 2020). Secondary hydration products such as AFt and C-S–H gel could fill the gaps and pores between fine aggregate and gel particles, forming a more compact system. In

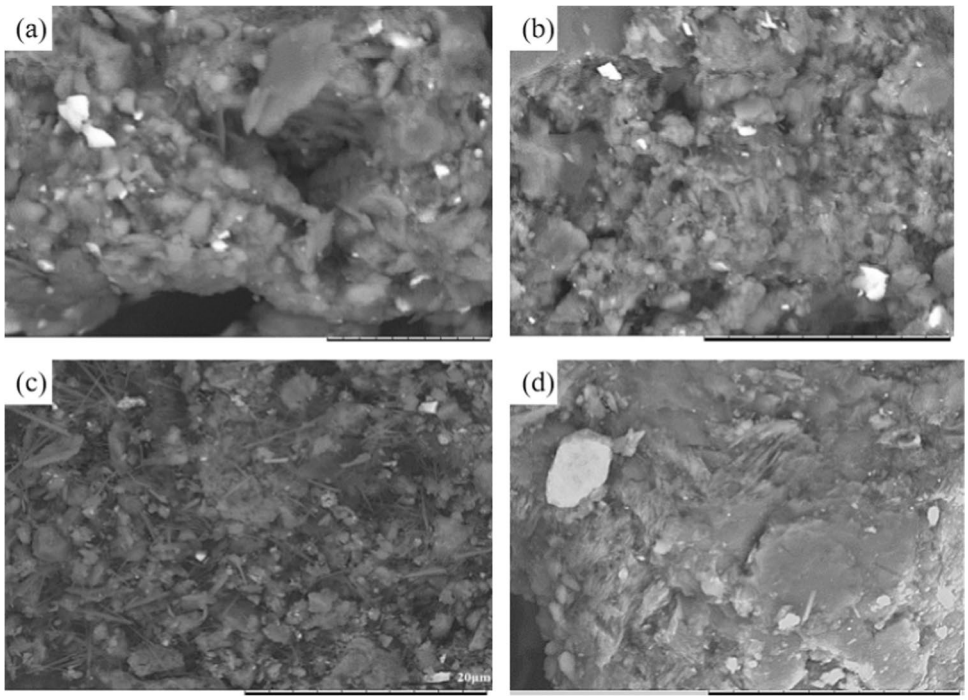

Fig. 7 SEM morphology of **a** WDC particle products with cement content of 6%, **b** WDC particle products with cement content of 8%, **c** WDC particle products with cement content of 10%, **d** WDC particle products with cement content of 12%

Table 15 Test results of WDC cushion leachate

Specimen	Test items	Result of survey	Unit	Test items	Result of survey	Unit
WDC cushion (50%)	Oil	0.04L	mg/L	Mercury	0.00014	mg/L
	Chemical oxygen demand (COD)	22	mg/L	Arsenic	0.0003L	mg/L
	Chloride	10.4	mg/L	Lead	0.002	mg/L
	Fluoride	5.60	mg/L	Cadmium	0.0001L	mg/L
	Nitrate nitrogen	22.5	mg/L	Barium	0.47	mg/L
	Hexavalent chromium	0.127	mg/L	Dibenzo(a,h) anthracene	0.002	mg/kg

addition, as the cement content increases from 6 to 10%, the diffraction peak of AFt gradually increases, but when the cement content reaches 12%, the diffraction peak intensity of AFt decreases slightly (Ciotoli et al. 2020; Antoniou and Antoniou 2019).

Based on the basic principle of the reaction of organic pollutants in WDC with cement, in order to better understand the interaction between WDC and volcanic ash materials, road cushion samples with different cement ratios were used to observe the microstructure of early hydration under SEM. The results are shown in Fig. 7, which are the microstructure of early hydration products of WDC samples when the cement ratios are 6%, 8%, 10%, and 12%, respectively. It can be seen from the figure that the particles of WDC are irregular, the particle surface is porous and loose, and the WDC particles are mostly lamellar (Okparanma et al. 2018; Demetriou et al. 2021). With the increase of cement content, the porosity of WDC particles decreases significantly. It indicates that doping appropriate WDC is conducive to the densification of the early microstructure of the system, and the existence of C-S–H and Aft generated by the secondary hydration of WDC is also confirmed by XRD analysis (Wang et al. 2019; Faried et al. 2021). The results show that the volcanic ash reaction of WDC generates a large number of AFt crystals interspersed in the C-S–H gel, so that the pores are filled to form a more compact microstructure. Therefore, under the same curing conditions, the microstructure of WDC sample is significantly optimized, so that it has higher durability and mechanical properties (Ghorbani et al. 2019; Jiang et al. 2020).

Environmental safety analysis of WDC cushion

The text results of WDC as cushion leaching solution are shown in Table 15. According to the text values of toxic substances in WDC as road cushion materials, the test results are analyzed. It can be obviously found that all the contents of substances

Table 16 Radioactive nuclide content in WDC

Type of drilling cuttings	^{232}Th Bq/kg	^{226}Ra	^{40}K	I_{Ra}	I_r
WDC	3.5×10^3	2.6×10^3	40×10^3	0.13	0.31

detected do not exceed the limit value of *Standards for irrigation water quality* (GB 5084–2021). At the same time, the contents of pollutants meet the standard limits of class I surface water in *Environmental quality standards for surface water* (GB 3838–2002), and the contents of heavy metals detected do not exceed the maximum allowable emission concentration of class I pollutants in *Integrated wastewater discharge standard* (GB 8978–1996). Therefore, WDC as road cushion materials meet the standard requirements (Han et al. 2020; Fu et al. 2019).

By comparing and analyzing the WDC to meet the reference limit of heavy metal content in raw materials of cement kiln cooperative disposal of solid waste into the kiln, at the same time as building materials, shale gas WDC as raw materials of cement industry must also meet the national standard of radioactivity of building materials (Allwood 2018). This index is usually used to measure the radioactivity of building materials by internal irradiation index I_{Ra} and external irradiation index I_r. The calculation formula is shown in (19) and (20). The results are shown in Table 16.

Mechanism analysis of cement solidifying organic pollutants in road cushion with WDC

Cement solidification is a common method to convert toxic and hazardous solid waste into non-hazardous substances. Cement is the most commonly used stabilizer for hazardous waste. The technology is to mix waste and cement to form a hard cement solidified body after hydration, so as to reduce the leaching of hazardous components in waste (Ciotoli et al. 2020). The process of cement curing organic pollutants is actually the process of interaction between organic pollutants and inorganic cementitious materials, and its interaction includes adsorption, chemical absorption, precipitation, ion exchange, and homocrystal substitution (Chen and Wu 2018; Guo et al. 2017).

The hydration process of WDC and cement is very complex, and the hydration products will change with the content of WDC. When the solidification products of WDC and cement contact with the leaching medium, the chemical equilibrium of the solidification products is broken due to the low concentration of chemical components in the medium (Cao et al. 2020). For the hydration products formed by hydration, the first is easy to dissolve to maintain the chemical equilibrium. For $Ca(OH)_2$, single sulfate, ettringite, C-S–H, and several hydration products, studies on their solubility indicate their solubility order, $Ca(OH)_2$ > single sulfate > AFt > ettringite > C-S–H, that is, $Ca(OH)_2$ is the most easy to dissolve, while ettringite and C-S–H are difficult to dissolve. From this point of view, these two hydration products play an important role in the solidification of organic pollutants (Mostavi et al. 2015; Tian et al. 2021).

Some organic pollutants in WDC mainly exist in the form of benzo(a)anthracene, benzo(k)fluoranthene, benzo(a)pyrene, and other polycyclic aromatic hydrocarbons. The presence of organic pollutants will not only interfere with the solidification and stabilization process of cement, but also change the strength of the product, making the stabilization process of pollutants more difficult (Xu et al. 2017). In general, organic compounds form a layer of organic compounds inhibiting hydration on the cement surface through ion bonds, hydrogen bonds, and dipole bonds. Through the adsorption of toxic substances by the powdery calcium silicate hydrated colloid in cement, the cementitious hydrate in cement and organic pollutants in WDC form a solid solution, so that the pollutants are bound in the cement hardening tissue, thereby greatly reducing the content of organic pollutants in WDC. The basic principle is to reduce the surface area and permeability of hazardous solidified organic polycyclic aromatic hydrocarbons by curing inclusion compounds, so as to achieve the purpose of stable and harmless organic pollutants (Ma et al. 2016; Bedia et al. 2018). The mechanism of cement solidification pollutants is shown in Fig. 8.

Process route of WDC as road cushion

Treatment process of WDC

The WDC process flow chart of road cushion is shown in Fig. 9, and the distribution construction steps are as follows:

Step 1 Stirring crushing and screening unit

The material is sent to the mixer by shovel truck, and then sent to the roller siever for screening. The material with particle size greater than 30 mm is screened out, and small particles enter the next unit.

Step 2 Stacking unit

Through the use of excavators and loaders, the screened solid waste is piled into a strip of 2 m wide and 0.5 m high.

Step 3 Flip and dosing unit

The solid waste is transmitted to the dump unit by conveyor belt, and the solid waste is dumped by hydraulic-assisted

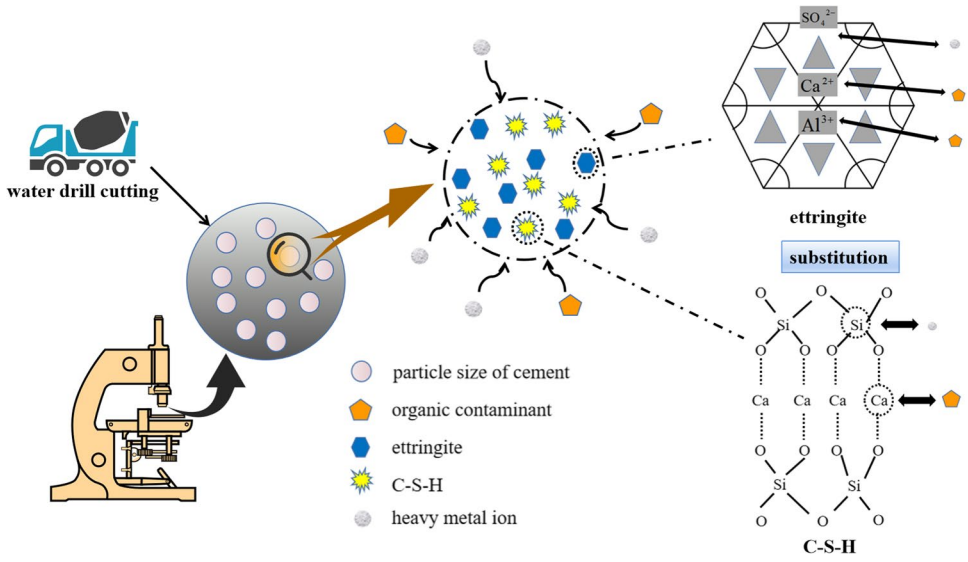

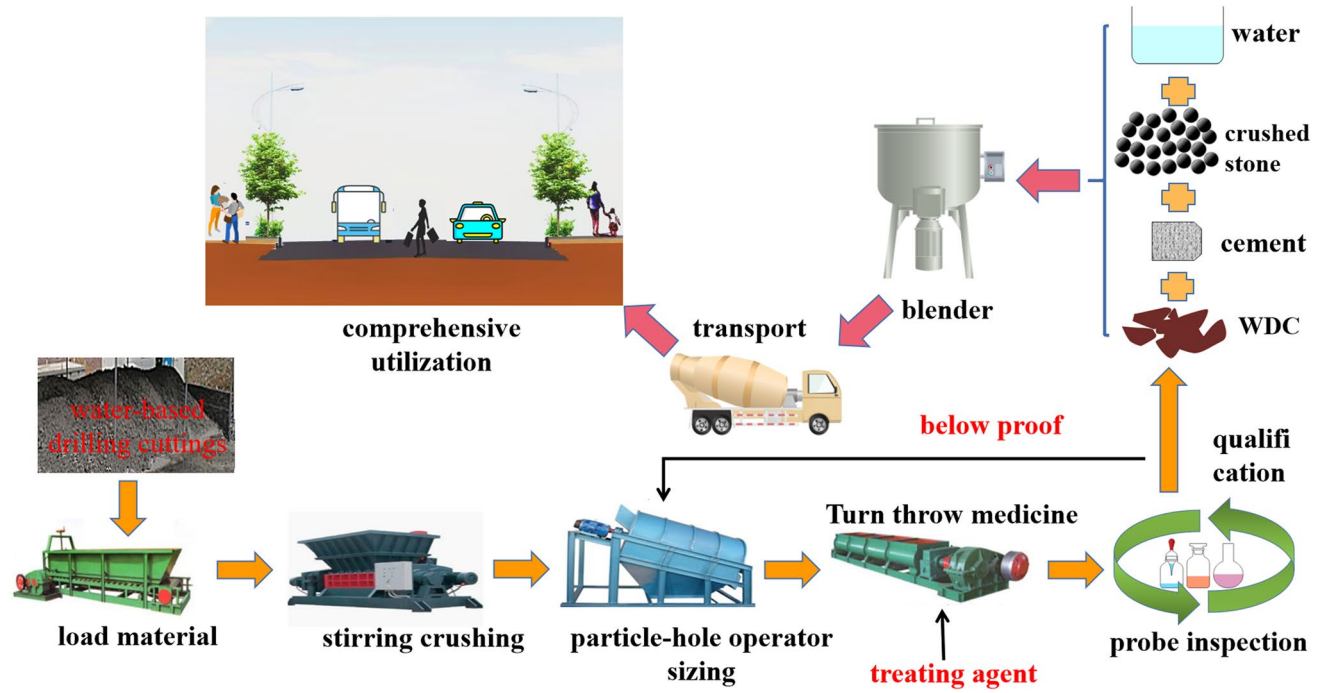

Fig. 8 Mechanism diagram of cement solidification pollutants

Fig. 9 WDC resource processing flow chart

mechanical crawler dumper. At the same time, the drug spraying equipment is used for uniform spraying. The dumper repeatedly dumps three to four times to make the drug evenly sprayed on the solid waste (Rodriguez et al. 2022).

Step 4 Material detection

After the material treatment was completed, it is detected that the qualified material entered the material stacking area, and the unqualified material is re-entered into the stacking tank for re-stacking.

WDC detection after treatment

The treated WDC should have no obvious irritating odor, and the pollutant content should meet the requirements in Table 16; WDC are used as road cushion and well site cushion pollution control requirements in the third chapter above. In addition, in order to further ensure the environmental safety of comprehensive utilization, the oil content of WDC is set to 0.3%.

Each 300 m^3 is used as a large sampling array for pollutant content detection.

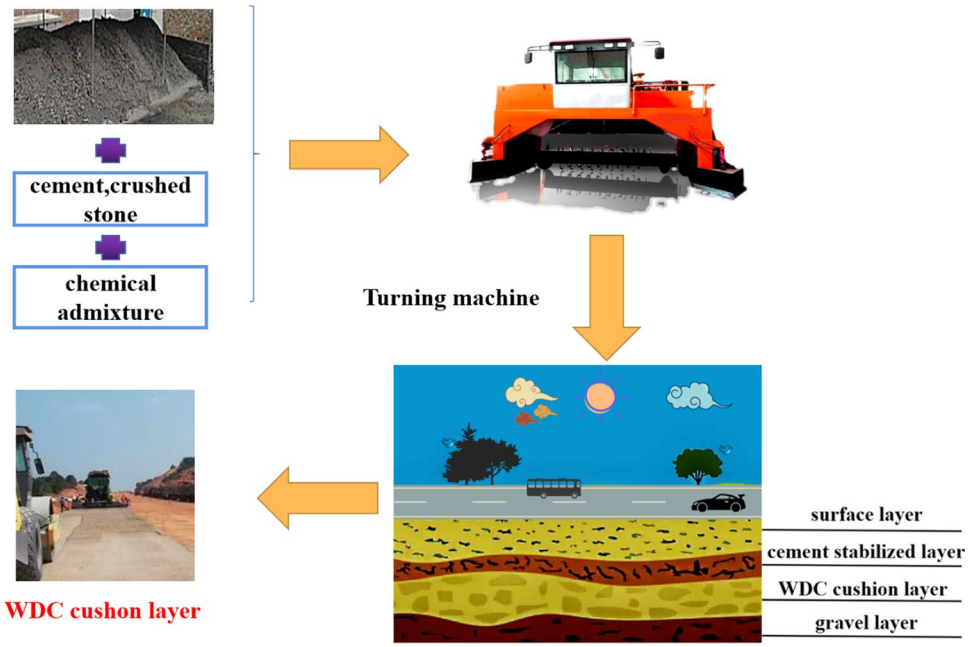

Fig. 10 WDC road cushion production process

Treatment of unqualified WDC: if the product is unqualified, it is necessary to re-do compound dosing treatment to meet the qualification requirements (Wang et al. 2018a, b, c, d).

Site layout

The production process of water-based drilling cuttings as road cushion is shown in Fig. 10.

Conclusions

The goal of this study is to experimentally evaluate the environmental performance and properties (including human health and ecological security risk assessment, mechanical, microstructural and environmental safety assessment) of the WDC and WDC road cushion. This study can provide a favorable way for the efficient, safe, and environmentally friendly utilization of WDC, and ensure the ecological environment safety and human health safety of WDC in resource utilization. The main results and conclusions are as follows.

The comprehensive carcinogenic risk of all exposure pathways of single pollutant benzo(a)anthracene, benzo(a)pyrene, benzo(k)fluoranthene, and indeno(1,2,3-cd)pyrene was acceptable. However, the cumulative carcinogenic risk of skin contact pathway of particulate matter intake of dibenzo(a,h)anthracene was at an unacceptable level. It was considered that only dibenzo(a,h) anthracene had carcinogenic effect, so the soil risk control value of heavy metals in WDC can be calculated: the risk control limit of dibenzo(a,h)anthracene in WDC was 1.8700 mg/kg.

In this study, cement solidification was used to convert organic pollutants in WDC into harmless substances. The basic principle was that organic substances form a layer of organic substances that inhibit hydration on the cement surface through ion bonds, hydrogen bonds, and dipole bonds. Through the adsorption of toxic substances by the powdery calcium silicate hydrated colloid in cement, the cementitious hydrate in cement and organic pollutants in WDC formed a solid solution, so that the pollutants were bound in the cement hardening tissue, thereby greatly reducing the content of organic pollutants in WDC.

By studying and adjusting the formula of WDC pavement cushion, the WDC pavement cushion was finally designed by 6% cement + 50% WDC + 44% crushed stone. The 28-day unconfined compressive strength met the requirements of the Chinese standard *Technical Guidelines for Construction of Highway Roadbases* (JTG/T F20-2015). The environmental protection, building materials, and safety of the product were sampled and analyzed. The leaching concentration of main pollutants met the relevant standards of China.

Annex 1

In this study, the Chinese standard *Technical guidelines for risk assessment of soil contamination of land for construcion* (HJ 25.3–2019) is used for human health and ecological security risk assessment. Table 17 shows the calculation results of leaching dilution factor LF_{gw} during the bedding utilization of WDC site, Table 18 shows the calculation results of groundwater drinking risk of WDC site, and Table 19 shows the calculation results of soil risk control value based on carcinogenic effect under different exposure conditions.

Table 17 Calculation results of leaching dilution factor LF_{gw} for bedding utilization in WDC field

Parameter name				Unit	Parameter value	Source of parameters
ρ_b	Volume weight of soil			kg/L	1.50	Guidelines for risk assessment
H′	Henry's constant	Benzo(a)anthracene		Zero dimension	4.91E-04	Guidelines for risk assessment
		Benzo(k)fluoranthene			2.39E-05	
		Benzo(a)pyrene			1.87E-05	
		Dibenzo(a,h)anthracene			5.76E-06	
		Indeno(1,2,3-cd)pyrene			6.56E-05	
θavs	Volume ratio of pore air in unsaturated soil			Zero dimension	0.12	RBCA Site Risk Assessment Model
θwvs	Volume ratio of pore water in unsaturated soil			Zero dimension	0.26	RBCA Site Risk Assessment Model
fom	Organic matter content			g•kg^{-1}	16.8	Actual measurement
Koc	Distribution coefficient of soil organic carbon/soil pore water		Benzo(a) anthracene	L•kg^{-1}	1.77E + 05	Guidelines for risk assessment
			Benzo(k) fluoranthene	L•kg^{-1}	5.87E + 05	Guidelines for risk assessment
			Benzo(a) pyrene	L•kg^{-1}	5.87E + 05	Guidelines for risk assessment
			Dibenzo(a,h) anthracene	L•kg^{-1}	1.91E + 06	Guidelines for risk assessment
			Indeno(1,2,3-cd)pyrene	L•kg^{-1}	3.47E + 06	Guidelines for risk assessment
K_S	Distribution coefficient of solute in soil and water		Benzo(a) anthracene	L•kg^{-1}	1.75E + 03	Calculation
			Benzo(k) fluoranthene	L•kg^{-1}	5.80E + 03	Calculation
			Benzo(a) pyrene	L•kg^{-1}	5.80E + 03	Calculation
			Dibenzo(a,h) anthracene	L•kg^{-1}	1.89E + 04	Calculation
			Indeno(1,2,3-cd)pyrene	L•kg^{-1}	3.43E + 04	Calculation
Ugw	Darcy rate of groundwater			cm·yr^{-1}	2.50E + 03	Guidelines for risk assessment
δgw	Thickness of groundwater mixed zone			m	2.00	Guidelines for risk assessment
P	Annual rainfall			mm	1400.00	Environment impact assessment statement
I_f	Permeability rate of water in soil			cm/a	30	Guidelines for risk assessment
Wgw	Length of contaminated area parallel to groundwater flow			m	45.00	Estimate

Table 17 (continued)

Parameter name			Unit	Parameter value	Source of parameters
L_1	Height of matting		m	1.00	Estimate
L_2	Groundwater depth		m	50.00	Report for risk assessment
LF_{gw}	Soil leaching dilution factor	Benzo(a) anthracene	kg/L	2.43E-06	Computation
		Benzo(k) fluoranthene	kg/L	7.33E-07	Computation
		Benzo(a) pyrene	kg/L	7.33E-07	Computation
		Dibenzo(a,h) anthracene	kg/L	2.25E-07	Computation
		Indeno(1,2,3-cd)pyrene	kg/L	1.24E-07	Computation

Table 18 Risk calculation results of drinking groundwater for bedding use in WDC field

Parameter name			Unit	Parameter value	Source of parameters
CGWERca	Exposure of drinking groundwater (Carcinogenic effect)		$L \bullet kg^{-1} \bullet d^{-1}$	4.19E-03	Computation
Cgw	Pollutant concentration in groundwater polluted by WDC	Benzo(a)anthracene	mg/L	8.26E-06	Computation
		Benzo(k)fluoranthene	mg/L	4.86E-05	Computation
		Benzo(a)pyrene	mg/L	6.99E-07	Computation
		Dibenzo(a,h)anthracene	mg/L	1.34E-06	Computation
		Indeno(1,2,3-cd)pyrene	mg/L	1.41E-07	Computation
SFo	Oral intake carcinogenic slope factor	Benzo(a)anthracene	$(mg \bullet kg^{-1} \bullet d^{-1})^{-1}$	7.30E-01	Guidelines for risk assessment
		Benzo(k)fluoranthene	$(mg \bullet kg^{-1} \bullet d^{-1})^{-1}$	7.30E-02	Guidelines for risk assessment
		Benzo(a)pyrene	$(mg \bullet kg^{-1} \bullet d^{-1})^{-1}$	7.30E + 00	Guidelines for risk assessment
		Dibenzo(a,h)anthracene	$(mg \bullet kg^{-1} \bullet d^{-1})^{-1}$	7.30E + 00	Guidelines for risk assessment
		Indeno(1,2,3-cd)pyrene	$(mg \bullet kg^{-1} \bullet d^{-1})^{-1}$	7.30E-01	Guidelines for risk assessment
WAF	Proportion of reference dose distribution exposed to groundwater		Zero dimension	0.20	Guidelines for risk assessment
CRcgw	Cancer Risk of Single Pollutant in Drinking Groundwater WDC	Benzo(a)anthracene	Zero dimension	2.53E-08	Computation
		Benzo(k)fluoranthene	Zero dimension	1.49E-08	Computation
		Benzo(a)pyrene	Zero dimension	2.14E-08	Computation
		Dibenzo(a,h)anthracene	Zero dimension	4.10E-08	Computation
		Indeno(1,2,3-cd)pyrene	Zero dimension	4.31E-10	Computation

Table 19 Soil risk control values based on carcinogenic effects

Parameter name			Unit	Parameter value	Source of parameters
ACR	Acceptable carcinogenic risk		Zero dimension	10^{-5}	Chongqing area
$OISER_{ca}$	Exposure of solid waste particles taken orally		$kg•kg^{-1}•d^{-1}$	4.19E − 07	Computation
DCSERca	Exposure of skin to WDC particles (carcinogenic effect)		$kg•kg^{-1}•d^{-1}$	3.11E − 07	Computation
PISERca	Exposure of inhaled dust particles (carcinogenic effect)		$kg•kg^{-1}•d^{-1}$	4.95E − 09	Computation
$RCVS_{ois}$	Soil risk control value based on carcinogenic effect of oral intake of soil pathway	Benzo(a)anthracene	$mg•kg^{-1}$	3.27E + 01	Computation
		Benzo(k)fluoranthene	$mg•kg^{-1}$	3.27E + 02	Computation
		Benzo(a)pyrene	$mg•kg^{-1}$	3.27E + 00	Computation
		Dibenzo(a,h)anthracene	$mg•kg^{-1}$	3.27E + 00	Computation
		Indeno(1,2,3-cd)pyrene	$mg•kg^{-1}$	3.27E + 00	Computation
$RCVS_{dcs}$	Soil risk control value based on carcinogenic effect of skin contact with soil pathway	Benzo(a)anthracene	$mg•kg^{-1}$	4.40E + 01	Computation
		Benzo(k)fluoranthene	$mg•kg^{-1}$	4.40E + 02	Computation
		Benzo(a)pyrene	$mg•kg^{-1}$	4.40E + 00	Computation
		Dibenzo(a,h) anthracene	$mg•kg^{-1}$	4.40E + 00	Computation
		Indeno(1,2,3-cd)pyrene	$mg•kg^{-1}$	4.40E + 01	Computation
$RCVS_{pis}$	Soil risk control value based on carcinogenic effect of inhaled soil particles	Benzo(a)anthracene	$mg•kg^{-1}$	4.70E + 03	Computation
		Benzo(k)fluoranthene	$mg•kg^{-1}$	4.70E + 03	Computation
		Benzo(a)pyrene	$mg•kg^{-1}$	4.70E + 02	Computation
		Dibenzo(a,h) anthracene	$mg•kg^{-1}$	4.30E + 02	Computation
		Indeno(1,2,3-cd)pyrene	$mg•kg^{-1}$	4.70E + 03	Computation

Annex 2

A total of WDC of three drilling platforms were leached and tested. The concentration test results are shown in Table 20. According to the standard limits of each leaching toxicity test item in the Chinese standard *Identification standards for hazardous wastes-Identification for extraction toxicity* (GB5085.3–2007), the pollutants in WDC were screened and the test results were analyzed. The toxic substances content of WDC as road cushion is detected, and the risk assessment of WDC as road cushion is carried out combined with the risk control limits in *Soil environmental quality-Risk control standard for soil contamination of agricultural land* (GB 15618–2018) and *Risk screening guideline values for soil contamination of development land (three drafts)* (HJ25.5–2015). In addition, the toxicity parameters and exposure parameters of the main pollutants required for the human health evaluation of WDC as road cushion are shown in Table 21 and Table 22.

Table 20 Detection values of toxic substances in WDC

Item (mg/kg)	A platform	B platform	C platform	D platform	E platform	F platform	G platform	*Soil environmental quality-Risk control standard for soil contamination of agricultural land* (GB 15,618–2018)	*Risk screening guideline values for soil contamination of development land (three drafts) (HJ 25.5–2015)*
Benzo(a)anthracene	0.7256	6.4978	1.4396	0.6987	0.3000	1.8329	0.9730	/	1.86
Benzo(k) fluoranthene	132.4004	3.2343	23.2822	8.6597	15.2000	0.1000	8.7025	/	18
Benzo(a)pyrene	0.0765	1.6071	0.1863	0.1000	0.1325	0.1726	0.0935	0.1	0.19
Indeno(1,2,3-cd)pyrene	1.5204	1.97	1.8300	0.3000	1.0973	0.5469	1.2596	/	1.87
Dibenzo(a,h) anthracene	0.1265	5.9552	0.1637	0.1324	0.1832	0.1754	0.0000	/	0.19
Benzo(ghi) perylene	ND	13.8816	ND	ND	ND	ND	ND	/	/

Table 21 Toxicity parameters of main pollutants

Name of pollutant	Benzo(a)anthracene	Benzo(k) fluoranthene	Benzo(a)pyrene	Dibenzo(a,h) anthracene	Source of parameters
Oral intake reference dose ($mg•kg^{-1}•d^{-1}$)	/	/	/	/	Guideline
Reference dose of skin contact ($mg•kg^{-1}•d^{-1}$)	/	/	/	/	Guideline
Reference dose of respiratory inhalation ($mg•kg^{-1}•d^{-1}$)	/	/	/	/	Guideline
Reference concentration of respiratory inhalation ($mg•m^{-3}$)	/	/	/	/	Guideline
Respiratory absorption efficiency factor (zero dimension)	1	1	1	1	Guideline
Oral intake carcinogenic slope factor $(mg•kg^{-1}•d^{-1})^{-1}$	7.30E-01	7.30E-02	7.30E + 00	7.30E + 00	Guideline
Skin contact carcinogenic slope factor $(mg•kg^{-1}•d^{-1})^{-1}$	7.30E-01	7.30E-02	7.30E + 00	7.30E + 00	Calculation
Respiratory inhalation carcinogenic slope factor $(mg•kg^{-1}•d^{-1})^{-1}$	4.30E-1	4.30E-1	4.30E + 00	4.70E + 00	Calculation
respiratory inhalation unit carcinogenic factor ($m^3•mg^{-1}$)	1.10E-01	1.10E-01	1.10E + 00	1.20E + 00	Guideline

Table 22 Selection of exposure parameters

Parameter symbolic	Parameter name	Unit	Recommended value of non-sensitive land	Remark
L_1	Cushion thickness	cm	100.00	Estimate
L_2	Groundwater depth	cm	1000.00	Estimate
ρ_b	Volume weight of soil	$kg·dm^{-3}$	1.50	Guideline
P_{ws}	Soil moisture content	$kg·kg^{-1}$	0.10	Guideline
h_v	Unsaturated zone thickness	cm	295.00	Estimate
i	Hydraulic slope	Zero dimension	0.01	Guideline
U_{gw}	Darcy rate of groundwater	$cm·a^{-1}$	2500.00	Guideline
W_{gw}	Length of soil pollution parallel to groundwater flow	cm	4500.00	Guideline
δ_{gw}	Thickness of groundwater mixed zone	cm	200.00	Guideline
EDa	Adult exposure cycle	a	25.00	Guideline
EFa	Adult exposure frequency	$d·a^{-1}$	250.00	Guideline
BWa	Average adult weight	kg	56.80	Guideline
Ha	Average height of adults	cm	156.30	Guideline
DAIRa	Daily air respiration of adults	$m^3·d^{-1}$	14.50	Guideline
OSIRa	Daily soil intake by adults	$mg·d^{-1}$	100.00	Guideline
Ev	Daily frequency of skin contact events	$meta·d^{-1}$	1.00	Guideline
SAF	Proportion of reference dose distribution exposed to soil	Zero dimension	0.20	Guideline
SERa	Surface area ratio of adult exposed skin	Zero dimension	0.18	Guideline
SSARa	Soil adhesion coefficient of adult skin surface	$mg·cm^{-2}$	0.20	Guideline
ABSo	Oral intake absorption efficiency factor	Zero dimension	1.00	Guideline
ABS_d	Skin Contact Absorption Efficiency Factor	Zero dimension	0.13	Guideline
PIAF	Inhaled particulate matter retention ratio in vivo	Zero dimension	0.75	Guideline
ACR	Single pollutant acceptable carcinogenic risk	Zero dimension	1.00E-06	Guideline
			1.00E-05	Chongqing area
AHQ	Acceptable non-carcinogenic risk	Zero dimension	1.00	Guideline
ATca	Average time of carcinogenic effect	d	26,280.00	Guideline
ATnc	Average time of non-carcinogenic effect	d	9125.00	Guideline

Author contribution Chao-qiang Wang: overall audit, experimental design, data and relevant mechanism analysis, writing—original draft. Shen Chen: assisting with research and experimentation, data and relevant mechanism analysis, revised and editing. De-ming Huang: assisting with experimental design, research, experiments, and data analysis. Qi-cong Huang: assisting with research and data analysis. Min-jie Tu: assisting with research and data analysis. Kai Wu: assisting with experimental design, research, and data analysis. Yan-yan Liu: assisting with research and data analysis. All authors read and approved the final manuscript.

Funding This work is funded by the Youth Project of Science and Technology Research program of Chongqing Education Commission of China (no. KJQN202100723), Opening Project of Key Laboratory of Solid Waste Treatment and Resource Recycle, Ministry of Education (20kfgk03), and Opening Project of Key Laboratory of Urban Pollutant Conversion, Chinese Academy of Sciences (KLUPC-KF-2020–2), Key Laboratory of Advanced Civil Engineering Materials (Tongji University), Ministry of Education (202103), Guangxi key Research and Development Program (Guike AB20159033), and Western Scholar of Chinese Academy of Sciences Category A(E2296201).

Data availability All data generated or analyzed during this study are included in this published article.

Declarations

Ethics approval This study does not contain any studies with human participants and/or animals.

Consent to participate Written informed consent was obtained from individual participants.

Consent to publish Not applicable.

Competing interests The authors declare no competing interests.

References

Abdul-Wahab SA, Al-Dhamr H, Ram G, Black L (2020) The use of oil-based mud cuttings as an alternative raw material to produce high sulfate-resistant oil well cement. J Clean Prod 269:122207

Allwood JM (2018) Unrealistic techno-optimism is holding back progress on resource efficiency. Nat Mater 17:1050–1051

Alves HPA, Junior RA, Campos LFA, Dutra RPS, Grilo JPF, Loureiro FJA (2017) Structural study of mullite based ceramics derived from a mica-rich kaolin waste. Ceram Int 43:3919–3922

Amin M, Zeyad AM, Tayeh BA, Agwa IS (2021) Effects of nano cotton stalk and palm leaf ashes on ultrahigh-performance concrete properties incorporating recycled concrete aggregates. Constr Build Mater 302:124196

Amelung W, Bossio D, de Vries W, Kogel-Knabner I, Lehmann J (2020) Towards a global-scale soil climate mitigation strategy. Nat Commun 11(1):5427

Antoniou N, Zorpas AA (2019) Quality protocol development to define end-of-waste criteria for tire pyrolysis oil in the framework of circular economy strategy. Waste Manag 95:161–170

Ayati B, Molineux C, Newport D, Cheeseman C (2019) Manufacture and performance of lightweight aggregate from waste drill cuttings. J Clean Prod 208:252–260

Ayati B, Ferrandiz-Mas V, Newport D, Cheeseman CR (2018) Use of clay in the manufacture of lightweight aggregate. Construct Build Mater 162:124–131

Ashwin NR, Christy PG (2017) Development of thermally efficient fibre-based eco-friendly brick reusing locally available waste materials. Constr Build Mater 133:275–284

Bamdad A, Chloe M, Darryl N, Christopher C (2019) Manufacture and performance of lightweight aggregate from waste drill cuttings. J Clean Prod 208:252–260

Ban CC, Ee TL, Ramli M (2018) The engineering properties and microstructure of sodium carbonate activated fly ash/slag blended mortars with silica fume. Compos B Eng 160:558–572

Baino F, Ferraris M (2019) Production and characterization of ceramic foams derived from vitrified bottom ashes. Mater Lett 236:281–284

Bedia J, Belver C, Ponce S, Rodriguez J, Rodriguez JJ (2018) Adsorption of antipyrine by activated carbons from FeCl3-activation of Tara gum. Chem Eng J 333:58–65

Boulicault JE, Alves S, Cole RB (2016) Negative ion MALDI mass spectrometry of Polyoxometalates (POMs): mechanism of singly charged anion formation and chemical properties evaluation. J Am Soc Mass Spectrom 27:1301–1313

Burghard Z, Andreas B, Wolf-Dieter S (2021) Recycling of Tungsten: Current share, economic limitations, technologies and future potential. Int J Refract Met H 98:105546

Burciaga-Díaz O, Durón-Sifuentes M, Díaz-Guillén J, Escalante-García J (2020) Effect of waste glass incorporation on the properties of geopolymers formulated with low purity metakaolin. Cem Concr Compos 107:103492

Cao Y, Liu R, Xu Y, Ye F, Xu R, Han Y (2019) Effect of SiO2, Al2O3 and CaO on characteristics of lightweight aggregates produced from MSWI bottom ash sludge (MSWI-BAS). Constr Build Mater 205:368–376

Cao Z, Rupert JM, Richard CL, Duan HB, Sacchi R, Zhou N, Reed MT, Jonathan MC, Ge QS, Liu G (2020) The sponge effect and carbon emission mitigation potentials of the global cement cycle. Nat Commun 11:3777

Chen C, Wu H (2018) Lightweight bricks manufactured from ground soil, textile sludge, and coal ash. Environ Technol 39(11):1359–1367

Chen W, Wang F, Li Z, Li Q (2020) A comprehensive evaluation of the treatment of lead in MSWI fly ash by the combined cement solidification and phosphate stabilization process. Waste Manag 114:107–114

Cheng XW, Long D, Zhang C, Gao XS, Yu YJ, Mei KY, Zhang CM, Guo XY, Chen ZW (2019) Utilization of red mud, slag and waste drilling flfluid for the synthesis of slag-red mud cementitious material. J Clean Prod 238:117902

Cheng G, Li Q, Su Z, Sheng S, Fu J (2018) Preparation, optimization, and application of sustainable ceramsite substrate from coal fly ash/waterworks sludge/oyster shell for phosphorus immobilization in constructed wetlands. J Clean Prod 175:572–581

China, General Administration of Quality Supervision, Inspection and Quarantine (1996) Integrated wastewater discharge standard, GB8978-1996

China, Ministry of Environment Protection (2015) Risk screening guideline values for soil contamination of development land (three drafts), HJ25.5-2015

China, Ministry of Transport (2015) Technical guidelines for construction of highway roadbases, JTG/T F20-2015

China, Ministry of Environment Protection (2016) Water quality-Determination of volatile organic compounds-Headspace/Gas chromatography mass spectrometry, HJ810-2016

China, Ministry of Ecological Environment (2018) State Administration for Market Regulation,Soil environmental quality-Risk

control standard for soil contamination of agricultural land, GB15618-2018
China, Ministry of Ecological Environment (2019a) Technical guidelines for risk assessment of soil contamination of land for construcion, HJ25.3-2019.
China, Ministry of Ecological Environment (2019b) Technical specifications on identification for hazardous waste, HJ/T298-2019
China, Ministry of Ecological Environment, State Administration for Market Regulation (2021) Standards for irrigation water quality, GB 5084-2021
China, State Environmental Protection Administration, General Administration of Quality Supervision, Inspection and Qurantine (2002) Environmental quality standards for surface water, GB3838-2002
Ciotoli G, Procesi M, Etiope G, Fracassi U, Ventura G (2020) Influence of tectonics on global scale distribution of geological methane emissions. Nat Commun 11:2305
Dai Z, Zhou H, Zhang W, Hu L, Huang Q, Mao L (2019) The improvement in properties and environmental safety of fired clay bricks containing hazardous waste electroplating sludge: The role of Na_2SiO_3. J Clean Prod 228:1455–1463
Danielle CSS, Auristela DM, Daniel AM, Carlos AP, Rubens MN (2019) Preparation of glass-ceramic materials using kaolin and oil well drilling wastes. J Mater Res Technol 8(4):3459–3465
Davarpanah A, Razmjoo A, Mirshekari B, Fantke P (2018) An overview of management, recycling, and wasting disposal in the drilling operation of oil and gas wells in Iran. Cogent Environ Sci 4:1537066
Demetriou E, Mallouppas G, Hadjistassou C (2021) Embracing carbon neutral electricity and transportation sectors in Cyprus. Energy 229:120625
Elmouwahidi A, Bailón-García E, Pérez-Cadenas AF, Maldonado-Hódar FJ, Carrasco-Marín F (2017) Activated carbons from KOH and H3PO4-activation of olive residues and its application as supercapacitor electrodes. Electrochim Acta 229:219–228
Fan C, Qian J, Yang Y, Sun H, Song J, Fan Y (2021) Green ceramsite production via calcination of chromium contaminated soil and the toxic Cr(VI) immobilization mechanisms. J Clean Prod 315:128204
Faried AS, Mostafa SA, Tayeh BA, Tawfik TA (2021) Mechanical and durability properties of ultra-high performance concrete incorporated with various nano waste materials under different curing conditions. J Build Eng 43:102569
Foroutan M, Hassan MM, Desrosiers N, Rupnow T (2018) Evaluation of the reuse and recycling of drill cuttings in concrete applications. Constr Build Mater 164:400–409
Fu Y, Shen Y, Zhang Z, Ge X, Chen M (2019) Activated biochars derived from rice husk via one-and two-step KOH-catalyzed pyrolysis for phenol adsorption. Sci Total Environ 646:1567–1577
George K, Antonis AZ (2021) Drill cuttings waste management from oil & gas exploitation industries through end-of-waste criteria in the framework of circular economy Strategy. J Clean Prod 322:129098
Ghorbani S, Ghorbani S, Tao Z, de Brito J, Tavakkolizadeh M (2019) Effect of magnetized water on foam stability and compressive strength of foam concrete. Constr Build Mater 197:280–290
Grilo JPF, Alves HPA, Araújo AJM, Andrade RM, Dutra RPS, Macedo DA (2019) Dielectric and electrical properties of a mullite/glass composite from a kaolinite clay/mica-rich kaolin waste mixture. Cerâmica 65:117–121
Guo B, Liu BO, Yang J, Zhang S (2017) The mechanisms of heavy metal immobilization by cementitious material treatments and thermal treatments: A review. J Environ Manage 193:410–422
Han R, Zhou B, Huang Y, Lu X, Li S, Li N (2020) Bibliometric overview of research trends on heavy metal health risks and impacts in 1989–2018. J Clean Prod 276:123249
Hossain MU, Wang L, Chen LT, Sang DCW, Mechtcherine V (2020) Evaluating the environmental impacts of stabilization and solidification technologies for managing hazardous wastes through life cycle assessment: a case study of Hong Kong. Environ Int 145:106–139
Hu G, Liu H, Chen C, Hou H, Li J, Hewage K, Sadiq R (2021) Low-temperature thermal desorption and secure landfill for oil-based drill cuttings management: pollution control, human health risk, and probabilistic cost assessment. J Hazard Mater 410:124570
Hu TR, Ji Y, Fei F, Zhu M, Jin TY, Xue P, Zhang N (2022) Optimization of COVID-19 prevention and control with low building energy consumption. Build Environ 219:109233
Issabayeva G, Hang SY, Wong MC, Aroua MK (2018) A review on the adsorption of phenols from wastewater onto diverse groups of adsorbents. Rev Chem Eng 34:855–873
Jiang N, Zhao YH, Shang KF, Lu N, Li J, Wu Y (2020) Degradation of toluene by pulse-modulated multistage DBD plasma: key parameters optimization through response surface methodology (RSM) and degradation pathway analysis. J Hazard Mater 393:122365
Kirchain JR, Gregory J, Olivetti E (2017) Environmental life-cycle assessment. Nat Mater 16:693–697
Lars H (1980) An ecological risk index for aquatic pollution control, a sedimentoligical approach. Water Res 14:975–1001
Li B, Wei S, Zhen YW (2020a) An effective recycling direction of water-based drilling cuttings and phosphogypsum co-processing in road cushion layer. Environ Sci Pollut R 27:17420–17424
Li LX, Annelise JB, John DS, Brent AC, Joel DS, Petros K (2020b) Unconventional oil and gas development and ambient particle radioactivity. Nat Commun 11:5002
Li R, Zhou Y, Li C, Li S, Huang Z (2019) Recycling of industrial waste iron tailings in porous bricks with low thermal conductivity. Constr Build Mater 213:43–50
Li SY, Wang Q, Jiang XT, Li RR (2022) The negative impact of the COVID-19 on renewable energy growth in developing countries: Underestimated. J Clean Prod 367:132996
Li Z, Ma Z, van der Kuijp TJ, Yuan Z, Huang L (2014) A review of soil heavy metal pollution from mines in China: pollution and health risk assessment. Sci Total Environ 468:843–853
Liu W, Yuan Y, Fan ZZ, Li J, Sun LR (2021) Using water-based drilling cuttings from shale gas development to manufacture sintered bricks: a case study in the southern Sichuan Basin, China. Environ Sci Pollut R 28:29379–29393
Loizia P, Voukkali I, Zorpas AA, Navarro PJ, Chatziparaskeva G, Inglezakis JV, Vardopoulos I (2021a) Measuring environmental performance in the framework of waste strategy development. Sci Total Environ 753:141974
Loizia P, Voukkali I, Chatziparaskeva G, Navarro PJ, Zorpas AA (2021b) Measuring the level of Environmental Performance on coastal environment before and during Covid-19 pandemic. A Case Study from Cyprus Sustainability-Basel 13:2485
Luo L, Li K, Fu W, Liu C, Yang S (2020) Preparation, characteristics and mechanisms of the composite sintered bricks produced from shale, sewage sludge, coal gangue powder and iron ore tailings. Constr Build Mater 232:117250
Ma B, Wang R, Ni H, Wang K (2019) Experimental study on harmless disposal of waste oil-based mud using supercritical carbon dioxide extraction. Fuel 252:722–729
Ma BG, Cai LX, Li XG, Jian SW (2016) Utilization of iron tailings as substitute in autoclaved aerated concrete: physico-mechanical and microstructure of hydration products. J Clean Prod 127:162–171
Maziar F, Marwa MH, Natalie D, Tyson R (2018) Evaluation of the reuse and recycling of drill cuttings in concrete applications. Evaluation of the reuse and recycling of drill cuttings in concrete applications. Constr Build Mater 164:400–409

Mohajerani A, Suter D, Jeffrey-Bailey T, Song T, Arulrajah A, Horpibulsuk S, Law D (2019) Recycling waste materials in geopolymer concrete. Clean Technol Envir 21(3):493–515

Mohsen P, Hamid H, Mohammad RE, Amir HH, Alireza B (2021) Obtaining the strength parameters of concrete using drilling data. J Build Eng 38:102–181

Mojoudi N, Mirghafari N, Soleimani M, Shariatmadari H (2019) Phenol adsorption on high microporous activated carbons prepared from oily sludge: equilibrium, kinetic and thermodynamic studies. Sci Rep-UK 9:19352

Mojtaba K, Leila M, Bahram D, Fereidoon MN, Ali K (2020) Reuse of drill cuttings in hot mix asphalt mixture: a study on the environmental and structure performance. Constr Build Mater 256:119–453

Moreno-Maroto JM, González-Corrochano B, Alonso-Azcárate J, Rodríguez L, Acosta A (2018) Assessment of crystalline phase changes and glass formation by rietveld-XRD method on ceramic lightweight aggregates sintered from mineral and polymeric wastes. Ceram Int 44(10):11840–11851

Mostavi E, Asadi S, Ugochukwu E (2015) Feasibility study of the potential use of drill cuttings in concrete. Procedia Eng 118:1015–1023

Mugahed AYH, Alyousef R, Alabduljabbar H, Khudhair MHR, Hejazi F, Alaskar A (2020) Performance properties of structural fibred-foamed concrete. Results Eng 5:100092

Muller G (1969) Index of geoaccumulation in sediments of the Rhime River. Geol J 2:109–118

Mymrin V, Alekseev K, Fortini OM, Aibuldinov YK, Pedroso CL, Nagalli A (2017) Environmentally clean materials from hazardous red mud, ground cooled ferrous slag and lime production waste. J Clean Prod 161:376–381

Notani MA, Moghadas NF, Fini EH, Hajikarimi P (2019) Low-temperature performance of toner-modified asphalt binder. J Trans Eng B: Pavements 145:4019022

Okparanma R, Araka P, Ayotamuno J, Mouazen A (2018) Towards enhancing sustainable reuse of pre-treated drill cuttings for construction purposes by near-infrared analysis: a review. J Civ Eng Constr Technol 9:19–39

Piszcz-Karaś K, Klein M, Hupka J, Łuczak J (2019) Utilization of shale cuttings in production of lightweight aggregates. J Environ Manag 231:232–240

Prachasaree W, Limkatanyu S, Hawa A, Sukontasukkul P, Chindaprasirt P (2020) Manuscript title: development of strength prediction models for fly ash based geopolymer concrete. J Build Eng 32:101704

Rehman S et al (2017) Simultaneous physisorption and chemisorption of reactive Orange 16 onto hemp stalks activated carbon: proof from isotherm modeling. Biointerface Res Appl Chem 7:2021–2029

Ren Q, Ren Y, Wu X, Bai W, Zheng J, Hai O (2019) Effects of pyrolusite and dolomite co-additives on the structure and properties of bauxite-based ceramics. Mater Chem Phys 230:207–214

Rodríguez-Li´ebana JA, Martín-Lara MA, Navas-Martos FJ, Penas-Sanjuan A, Godoy V, Arjandas S, Calero M (2022) Morpho-structural and thermo-mechanical characterization of recycled polypropylene and polystyrene from mixed post-consumer plastic waste. J Environ Chem Eng 10:108332

Roy A, Stegemann JA (2017) Nickel speciation in cement-stabilized/solidified metal treatment filtercakes. J Hazard Mater 321:353–361

Salari M et al (2019) High performance removal of phenol from aqueous solution by magnetic chitosan based on response surface methodology and genetic algorithm. J Mol Liqs 285:146–157

Sean WDT, Jennie SR, Kristian DN, Chris RV, Ryan M, Kerim D, Landon M (2021) Comparison of potential drinking water source contamination across one hundred U.S. cities. Nat Commun 12:7254

Senneca O, Cortese L, Martino RD, Fabbricino M, Ferraro A, Race M, Scopino A (2020) Mechanisms affecting the delayed efficiency of cement-based stabilization/ solidification processes. J Clean Prod 261:121–230

Shao YY, Shao YQ, Zhang WY, Zhu Y, Dou T, Chu LZ, Liu ZD (2022) Preparation of municipal solid waste incineration fly ash-based ceramsite and its mechanisms of heavy metal immobilization. Waste Manage 143:54–60

Siddique S, Leung SP, Njuguna J (2021) Drilling oil-based mud waste as a resource for raw materials: a case study on clays reclamation and their application as fillers in polyamide 6 composite. Upstream Oil and Gas Techonl 7:100036

Stoch P, Ciecińska M, Stoch A, Kuterasiński U, Krakowiak I (2018) Immobilization of hospital waste incineration ashes in glass-ceramic composites. Ceram Int 44:728–734

Sundis MST, Shireen TS, James HH, Bassam AT (2021) Behavior of geopolymer concrete deep beams containing waste aggregate of glass and limestone as a partial replacement of natural sand. Case Stud Constr Matc 15:e00744

Sun Y, Li JS, Chen Z, Xue Q, Sun QI, Zhou Y, Chen X, Liu L, Poon CS (2021) Production of lightweight aggregate ceramsite from red mud and municipal solid waste incineration bottom ash: Mechanism and optimization. Constr Build Mater 287:122993

Symeonides D, Loizia P, Zorpas AA (2019) Tires waste management system in Cyprus in the framework of circular economy strategy. J Environ Sci Pol Res 26:35445–35460

Tajuelo RE, Anovitz LM, Clement CD, Rondinone AJ, Cheshire MC (2018) Facile emulsion mediated synthesis of phase-pure diopside nanoparticles. Sci Rep 8(1):3099

Tian X, Rao F, Li C, Ge W, Lara NO, Song S, Xia L (2021) Solidification of municipal solid waste incineration fly ash and immobilization of heavy metals using waste glass in alkaline activation system. Chemosphere 283:131240

Tsangas M, Jeguirim M, Limousy L, Zorpas A (2019) The application of the application of analytical hierarchy process in combination with PESTEL-SWOT analysis to assess the hydrocarbons sector in Cyprus. Energies 12:791

Voukali I, Loizia P, Navarro PJ, Zorpas AA (2021) Urban strategies evaluation for waste management in coastal areas in the framework of area metabolism. Waste Manag Res 39(3):448–465

Wang CQ, Xiong DM (2021) Leaching assessment of aerated concrete made of recycled shale gas drilling cuttings: Particular pollutants, physical performance and environmental characterization. J Clean Prod 282:125099

Wang CQ, Lin XY, Mei XD, Luo XG (2019) Performance of non-fired bricks containing oil-based drilling cuttings pyrolysis residues of shale gas. J Clean Prod 206:282–296

Wang CQ, Lin XY, Wang D, He M, Zhang SL (2018a) Utilization of oil-based drilling cuttings pyrolysis residues of shale gas for the preparation of nonautoclaved aerated concrete. Constr Build Mater 162:359–368

Wang CQ, Lin XY, Chun Z, Xu DM (2017a) A study on the oilbased drilling cuttings pyrolysis residues resource utilization by the exploration and development of shale gas. Environ Sci Pollut Res 24(21):17816–17828

Wang CQ, Lin XY, Chun Z, Xu DM (2017b) Environmental security control of resource utilization of shale gas' drilling cuttings containing heavy metals. Environ Sci Pollut Res 24(27):21973–21983

Wang Q, Su M (2020) A preliminary assessment of the impact of COVID-19 on environment-A case study of China. Sci Total Environ 728:138915

Wang Q (2021) Zhang FZ (2021) What does the China's economic recovery after COVID-19 pandemic mean for the economic growth and energy consumption of other countries? J Clean Prod 295:126265

Wang Q, Chen X, Awadhesh NJ, Howard R (2014) Natural gas from shale formation-The evolution, evidences and challenges of shale gas revolution in United States. Renew Sust Energ Rev 30:1–28

Wang Q, Li SY, Li RR, Ma ML (2018) Forecasting U.S. shale gas monthly production using a hybrid arima and metabolic nonlinear grey model. Energy 07:047

Wang L, Chen L, Tsang DCW, Li J, Poon CS, Baek K, Hou DY, Ding SM (2018c) Recycling dredged sediment into fill materials, partition blocks, and paving blocks: technical and economic assessment. J Clean Prod 199:69–76

Wang JY, Yuan J, Xiao FP, Li ZZ, Wang J, Xu ZZ (2018d) Performance investigation and sustainability evaluation of multiple-polymer asphalt mixtures in airfield pavement. J Clean Prod 189:67–77

Wang YQ, Bai Y, Wang JY (2016) Distribution of urban soil heavy metal and pollution in different functional zones of Yinchuan City. Energ Environ Sci 37(2):710–716

Xiao R, Ma Y, Jiang X, Zhang M, Zhang Y, Wang Y, Huang B, He Q (2020) Strength, microstructure, efflorescence behavior and environmental impacts of waste glass geopolymers cured at ambient temperature. J Clean Prod 252:119610

Xie T, Visintin P, Zhao X, Gravina R (2020) Mix design and mechanical properties of geopolymer and alkali activated concrete: review of the state-of-the-art and the development of a new unified approach. Constr Build Mater 256:119380

Xu H, Song W, Cao W, Shao G, Lu H, Yang D, Chen D, Zhang R (2017) Utilization of coal gangue for the production of brick. J Mater Cycles Waste Manag 19(3):1270–1278

Yang J, Wang G, Wang D, Zhang Z (2017) A self-cleaning coating material of TiO_2 porous microspheres/cement composite with high-efficient photocatalytic depollution performance. Mater Lett 200:1–5

Yang SZ, Yao XL, Li JW, Wang XJ, Zhang C, Wu S, Wang K, Wang WL (2021) Preparation and properties of ready-to-use low-density foamed concrete derived from industrial solid wastes. Constr Build Mater 287:122946

Ye J, Hu A, Ren G, Zhou T, Zhang G, Zhou S (2017) Red mud enhances methanogenesis with the simultaneous improvement of hydrolysis-acidification and electrical conductivity. Bioresour Technol 247:131–137